SAHC

The assessment of the water transport in the soil-masonry complex of the 18th century churches

Joe Chalhoub

Czech Republic | 2020

ADVANCED MASTERS IN STRUCTURAL ANALYSIS OF MONUMENTS AND HISTORICAL CONSTRUCTIONS

Master's Thesis

Joe Chalhoub

The assessment of the water transport in the soil-masonry complex of the 18th century churches.

University of Minho

Czech Republic | 2020

Master's Thesis

Joe Chalhoub

The assessment of the water transport in the soil-masonry complex of the 18th century churches.

Czech Republic | 2020

CZECH TECHNICAL UNIVERSITY IN PRAGUE
Faculty of Civil Engineering
Thákurova 7, 166 29 Prague 6, Czech Republic

DIPLOMA THESIS ASSIGNMENT FORM

I. PERSONAL AND STUDY DATA

Surname: Chalhoub Name: Joe Personal number: 497052

Assigning Department: Department of Landscape Water Conservation

Study programme: Civil Engineering

Branch of study: Advanced Masters in Structural Analysis of Monuments and Historical Construction

II. DIPLOMA THESIS DATA

Diploma Thesis (DT) title: The assessment of the water transport in the masonry-soil complex of the 18th century churches

Diploma Thesis title in English: see above

Instructions for writing the thesis:
The goal of the dissertation is to assess water migration paths from soil to masonry of the 18th-century church of All Saints (in Hermankovice) or church of the St. Anna (in Viznov). The churches belong to Broumov Group of Churches – a unique part of the cultural heritage of the Czech Republic. Both churches are located on a hillslope, where the shallow subsurface runoff contributes to the elevated and fluctuating moisture levels of soil around and below of footing masonry. This condition is responsible for the degradation of the foundations with a consequently reduced bearing capacity of the walls. Raised moisture of masonry additionally causes the growth of algae and overall deterioration of the plaster in the church interior. Moisture transport in the foundations and surrounding soil has been monitored since 2016 in Hermankovice and 2017 in Viznov in an automated system consisting of water potential and moisture sensors.
The aim of this thesis is to analyze and synthesize the data from the monitoring system with consideration of the weather and geophysical data. Suggest hypotheses of the transport of water into masonry. Perform numerical modelling of the water transport in the masonry for a more advanced data interpretation. Based on the detailed assessment recommend the most suitable measures to reduce the water-related degradation of the churches under the study.

List of recommended literature:
T. Vogel, J. Dusek, M. Dohnal, and M. Snehota, “Moisture regime of historical sandstone masonry — A numerical study,” J. Cult. Herit. 42 99–107, 2019
Other articles in scientific journals listed in Web of Science.

Name of Diploma Thesis Supervisor: Michal Sněhota

DT assignment date: April 6, 2020 DT submission date: July 12, 2020

DT Supervisor’s signature Head of Department’s signature

III. ASSIGNMENT RECEIPT

I declare that I am obliged to write the Diploma Thesis on my own, without anyone’s assistance, except for provided consultations. The list of references, other sources and consultants’ names must be stated in the Diploma Thesis and in referencing I must abide by the CTU methodological manual “How to Write University Final Theses” and the CTU methodological instruction “On the Observation of Ethical Principles in the Preparation of University Final Theses”.

Assignment receipt date Student’s name

DECLARATION

Name: Joe Chalhoub

Email: Joe_chalhoub@hotmail.com

Title of the Msc Dissertation: The assessment of the water transport in the masonry-soil complex of the 18th century churches

Supervisor(s): doc. Ing. Michal Snehota Ph.D.

Year: 2020

I hereby declare that all information in this document has been obtained and presented in accordance with academic rules and ethical conduct. I also declare that, as required by these rules and conduct, I have fully cited and referenced all material and results that are not original to this work.

I hereby declare that the MSc Consortium responsible for the Advanced Masters in Structural Analysis of Monuments and Historical Constructions is allowed to store and make available electronically the present MSc Dissertation.

University: Czech Technical University in Prague

Date: 12/07/2020

Signature: _____

This page is left blank on purpose.

ACKNOWLEDGEMENTS

First of all, I would like to begin by thanking the SAHC Consortium that allowed me to participate to this Master. A special word of thanks to all the professors in the University of Minho that, with their knowledge, helped me elaborate difficult subjects such as historical constructions.

In addition, I offer my deepest gratitude to all the people who have supported me in this work, my parents and friends who have always been present with their encouragement and moral support throughout this journey. Furthermore, it is a pleasure to thank my supervisor, Dr. Michal Snehota, who contributed greatly to the realization of this project, for his encouragement and follow-up when necessary.

Finally, I would also like to mention Mrs. Alexandra Kurfurstova and Prof. Petr Kabele for assisting with administrative matters with regards to the university and allowing me to focus on thesis during these periods.

This page is left blank on purpose.

ABSTRACT

The study deals with the transport of water in the masonry and in the surrounding soil of the All Saints Church in Heřmánkovice and the Church of St. Anna in Vižňov. Part of this thesis consists of a review of available studies on the subject and a broader description of both sites. Water content, water potential and temperatures were evaluated for both sites using data from sensor systems installed in the northern walls of the churches made from sandstone which are most threatened by moisture, and in the soil in the vicinity of each church. These evaluated data, were filtered and merged from many measurement periods starting in 2016 for All Saints church and 207 for St. Anna's church. Clear evidences of the link between changes in masonry water content and potential with changes in the surrounding environment such as temperature and precipitation were found in the measured data. In addition, numerical modelling of water transport in the masonry is carried out for further interpretation of the data. Finally, on the basis of the detailed assessment, the most appropriate measures to reduce water-related degradation of the churches under study are recommended.

Key words: masonry, moisture, water content, water potential, water transport.

This page is left blank on purpose.

ABSTRAKT

Studie se zabývá transportem vody ve zdivu a zemině v okolí základů kostela Všech svatých v Heřmánkovicích a kostela sv. Anny ve Vižňově. Součástí této práce je přehled dostupnéliteratury na témata dotýkající se vlhkosti zdiva historických staveb a širší popis lokalit. Měření vlhkosti a vodního potenciálu byla vyhodnocena pro obě v lokalitya základě dat ze senzorových systémů instalovaných v severní zdi kostelůa v půdě severně od kostelů. Tato vyhodnocená data byla filtrována a sloučena z mnoha období měření počínaje rokem 2016 pro kostel Všech svatých a 2017 pro kostel sv. Anny. V naměřených hodnotách bylo nalezeno několik jasných důkazů o souvislostech mezi změnami v vlhkosti ve zdi a změnami vlhkosti okolního prostředí. Dále bylo provedeno numerické modelování proudění vody ve zdivu pro rozšíření interpretace dat. Nakonec se na základě podrobného posouzení doporučují nejvhodnější opatření ke snížení degradace studovaných kostelů v důsledku působení vody.

Klíčová slova: zdivo, vlhkost, obsah vody, vodní potenciál, transport vody.

This page is left blank on purpose.

RESUMÉ

L'étude porte sur le transport de l'eau dans la maçonnerie et dans le sol environnant de l'église de Tous les Saints (Heřmánkovice) et de l'église St. Anna (Vižňov). Une partie de cette thèse consiste en un examen des études disponibles sur le sujet et une description plus large des deux sites. La teneur en eau, le potentiel hydrique et les températures ont été évalués pour les deux sites à l'aide de données provenant de systèmes de capteurs installés dans les murs nord des églises en pierre de sable, qui sont les plus menacés par l'humidité, et dans le sol à proximité de chaque église. Ces données évaluées, ont été filtrées et fusionnées à partir de nombreuses périodes de mesure à partir de 2016 pour l'église de Tous les Saints et de 2017 pour l'église St. Anna. Les données mesurées ont mis en évidence le lien entre les changements de la teneur en eau de la maçonnerie et le potentiel avec les changements du milieu environnant, tels que la température et les précipitations. En outre, une modélisation numérique du transport de l'eau dans la maçonnerie est effectuée pour une interprétation plus approfondie des données. Enfin, sur la base de l'évaluation détaillée, les mesures les plus appropriées pour réduire la dégradation liée à l'eau des églises étudiées sont recommandées.

Mots clés : maçonnerie, humidité, teneur en eau, potentiel hydrique, transport de l'eau.

This page is left blank on purpose.

TABLE OF CONTENTS

LIST OF FIGURES

LIST OF TABLES

This page is left blank on purpose.

1. INTRODUCTION

The All Saints church in Heřmánkovice and the Saint Anna church in Vižňov belong to the Broumov group of churches which is a unique grouping of eleven baroque churches built in the first half of the 18th century by Kryštof and Kilián Ignác Dientzenhofer. These two baroque churches are a unique part of the cultural heritage of Czech Republic and are made from sandstones. The two structures are located on hill slopes where the shallow subsurface runoff contributes to the elevated and fluctuating moisture levels of soil around and below of the masonry.

The assessment the water transport coming from the soil and affecting the integrity of the church of All Saints in Heřmánkovice and the Saint Anna church in Vižňov needs to be done. To carry out this assessment it is important to know the history and the actual condition of the churches, along with a literature review regarding moisture in historical buildings. Also, the analysis of the data from the monitoring system regarding water content levels and water potential. Furthermore, the modelling of water transport inside the walls of the churches would provide more information to interpret the water transport.

This page is left blank on purpose.

2. AIM OF WORK

The aim of this work is to evaluate the movement of water from the soil to the masonry of the 18th century Baroque Church of All Saints (in Heřmánkovice) and the Church of St. Anna (in Vižňov). The partial objectives are to research the available sources dealing with this phenomenon, to evaluate the results of monitoring in the locality, to carry out numerical modelling of water transport in the masonry for further interpretation of the data and to propose possible solutions to the unsatisfactory state of the structures.

This page is left blank on purpose.

3. HISTORY

It is important to research the contexts in which the building is constructed before working in cultural heritage. These include the time of construction, the location and the important persons involved in the construction, such as the constructor and the user. Historical building survey is a way to learn in depth about the state of conservation of a building or a group of buildings and their historical growth – otherwise speaking, to find out which of the standing sections are the oldest, and when they were constructed, what the building looked like at the time, how it developed slowly, or, conversely, what sections of it were lost. [1]

Understanding these aspects makes it easier to fully appreciate the significance of the construction, the structural methods employed in the construction, as well as potential causes of damages in its history.

3.1 History of Bohemia

The Duchy of Bohemia was a monarchy and part of the Holy Roman Empire in central Europe during the middle ages (Figure 1). During the 12th century the Kingdom of Bohemia was established by the duchy of Bohemia, it is the precursor to the modern known Czech Republic.

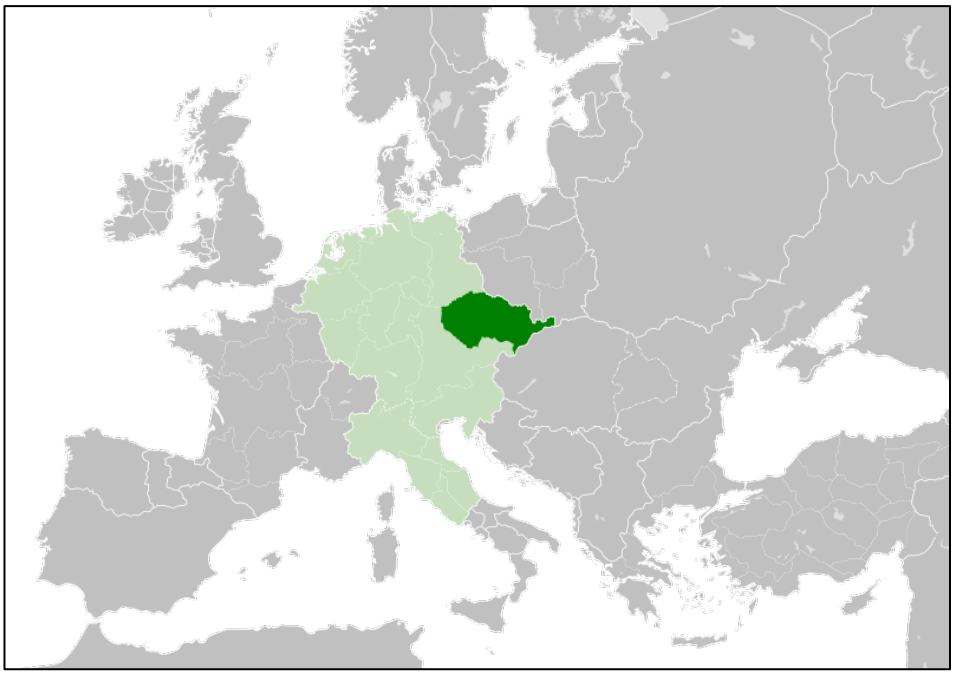

Figure 1 The Duchy of Bohemia and the Holy Roman Empire in 11th century [2]

During the reign of King Přemysl Otakar II between 1253 and 1278 Austria, Styria, Carinthia, and Carniola were acquired (Figure 2). Thus the Bohemian Kingdom is expanding towards the Adriatic Sea. After that, the Polish crown was acquired by Ottokar's son, Wenceslas II, and the Hungarian crown was also acquired for his son in 1300. The great Bohemian empire stretched from the Baltic sea

to the Danube river. After the death of Wenceslas III and several genealogical wars, the house of Luxembourg gained the Bohemian crown.

Figure 2 Lands ruled by Ottokar II in 1273

The golden age of Czech history is dated to the 14th century when Karel IV from the Luxembourg House became the king of Germany and the Holy Roman empire. The founding of Charles University in Prague in 1348, Charles Bridge, Charles Square, were of special importance.

The son of Charles IV, Wenceslas IV, succeeds him as King of Germany, but is then unworthy of the succession that his father had arranged for him. Throughout a long reign, he lost control of both Germany and Bohemia, including the Hussite declining rule of the Bohemian monarchy, until the fall of the Catholic Habsburg Empire in the 16th century.

The 17th century spotted several events that will affect Bohemia starting with the Defenestration of Prague in1618 where two Hapsburg-appointed Catholic rulers were forcefully thrown out of the Hradčany fortified palace windows. This occurrence sparked the developments that led to the thirty years war between Protestants and Catholics in Central Europe.[3]

The Broumov group of churches was built at the beginning of the 18th century as Bohemia started to emerge from the destruction done by the war where most of the infrastructure was wiped out between 1618 and 1648.

3.2 Bohemian Baroque

Baroque architecture began in Italy at the beginning of the 17th century with the Catholic Church, particularly the Jesuits, in order to bring people back to Christianity with a new architectural form. The new architecture of the churches was designed in a way that appeals to feelings in order to win the confidence and faith of the subjects of the Catholic Church. An example of the latest style is the church of the Gesù in Rome, built between 1568 and 1584, which had a single nave and no aisles to concentrate on the altar.[4]

Central European baroque emerged in the second half of the 17th century and was inspired by the Roman baroque. The propagation of the baroque style was combined with the triumph of the Catholic Church in the Thirty Years War, which made the Catholic Church the legitimate church of Bohemia, beginning in 1627.

A significant period of the bohemian baroque is the high baroque, also known as the radical baroque, which started in 1690 and continued until the middle of the 18th century. The most important architects of this time were Christoph Dientzenhofer, originally from Bavaria and living in Prague, and his son, Kilian Ignaz Dientzenhofer. the so-called radical baroque style was influenced by northern Italy and characterized by the combination of oval spaces and the curvature of walls. Together they constructed the Church of St. Nicholas in the Lesser Town of Prague, which became one of the most significant baroque churches in Europe. It was in this style that the Broumov group of churches were designed.[5]

3.3 Broumov Region

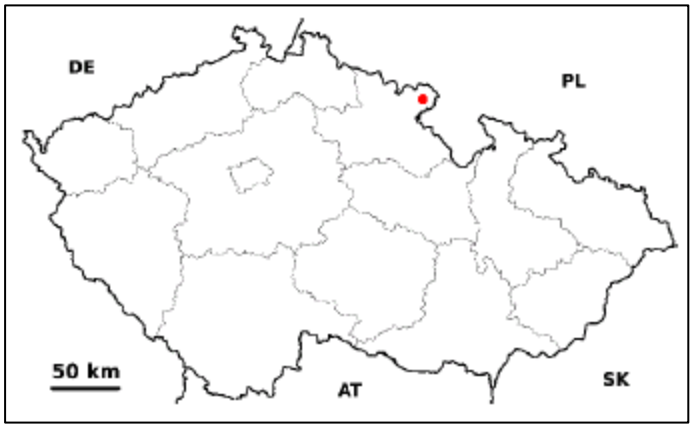

Figure 3 Broumov Region within Czech Republic

The Broumov region is a geographically and historically distinct area with a visually captivating landscape. During the administration of the Benedictine monks exquisite monuments and structures

were constructed, which made this region a very significant cultural center over many centuries. The landscape consists of mountains, valleys, bizarre rock formations, mosaics of forestland, meadows and grassland. The unique location of the place along with its scenic landscape, the magnificent architecture seen in the churches and monuments, make this area exceptional. it creates a “genius loci” – spirit of this place – that makes Broumov a captivating region (Figure 3).

This region was settled in the 13th century by the Benedictine order of Brevnov and the land was given to them by the bohemian king Premysl Otakar I. In the towns of Broumov and Police nad Metuji are two Benedictine monasteries and after the building of the monasteries the monks started bringing people and settled in small villages near water sources.

Owing to its position and diverse community, this region has undergone multiple political and religious crises. This involves disputes between Catholics and Protestants, Thirty Years Wars, and plagues. However, it has also managed to restore itself due to the strong economic condition and commercial practices of the Benedictine abbey. In the wake of the Thirty Years' War in the 18th century, the region saw a massive restoration of the monasteries and new constructions of Baroque stone churches, replacing existing wooden churches by the abbot's order. In the 19th century, the city experienced great wealth as a consequence of the growth of the textile industry and political freedom. This was demonstrated by the population boom and the building of sacred places of architectural values in the surrounding areas.

The 20th century has taken with it tragic years. The plurality of people of German descent rejected Czechoslovakia citizenship. Many protests were trimmed by the economic problems of the 1930s. The Henlein Party was established in 1933 and, after the Munich Agreement, the Broumov Area became divided — Broumov and Teplice became part of Hitler's Third Reich, and the Police became part of the Bohemia Protectorate — Moravia. The total breakdown of Broumov's growth came after the Second World War. After the war, German inhabitants who did not swear loyalty to Czechoslovakia were expelled from the country. The communist philosophy that proceeded started to kill the traditional heritage. Businesses and cultivation have been nationalized and socialist villages have been created. The city of Broumov and its community has been dissolved.[6]

3.4 Broumov Group of Churches

The baroque churches built in the region of Broumov form a unique architectural landmark for the region. The so-called "Broumov Group" are built on the territory of the Broumov monastic estate based on the designs and plans of Christoph Dientzenhofer and his son Kilian Ignaz. They were built in a very short period of time between 1709 & 1743 and are the result of an economic growth. The ten country churches are unique and of a creative originality which make part of the bohemian radical

baroque (Figure 4). Construction was started due to the insufficient network of old wooden churches and was initiated by abbot Otmar Zinke a very capable provost of the Benedictine monastery.[7]

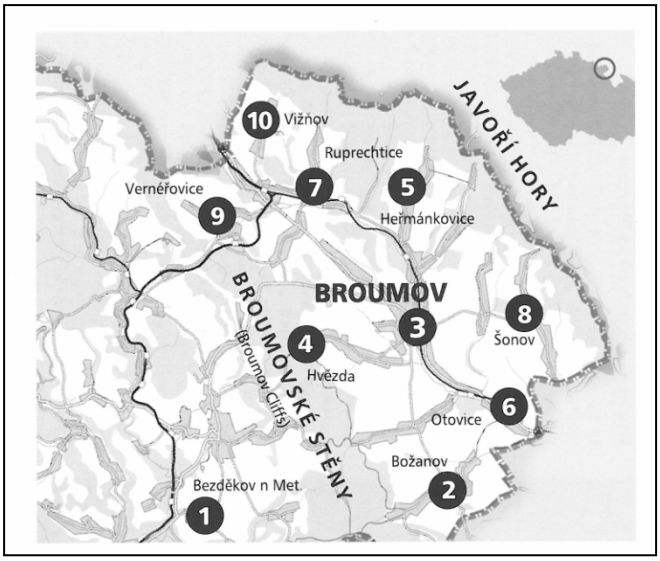

Figure 4 Broumov Group of Churches Map View [8]

3.5 All Saints Church, Heřmánkovice

The All Saints' Church was founded to substitute the presence of a timber church established in 1672 by the abbot Thomas Sartorius as the only holy place in the community. The new church is located on a hill above the village and dominates the local countryside. Kilian Ignaz Dientzenhofer was selected by Abbot Otmar Zinke to be the builder of this structure and had the shell construction finished in 1723, although the interior of the church lasted three more years (Figure 5).

Figure 5 All Saints Church - Hermankovice

The floor plan of the church is an octagon with curved walls. The organ loft is situated next to a tower with rounded corners. There is a small chancel at the end of the body of the building and a rectangular sanctuary behind it. The combination of the tall bell tower and the high roof created a monumental impact of the structure. The ceiling of the church is painted with a view to the heavens, also the painting portraits of the four evangelists are painted in semicircular fields with angels in elliptical bracings. The original painting was done after the building was completed, but had to be painted again 1865 (Figure 6).[7]

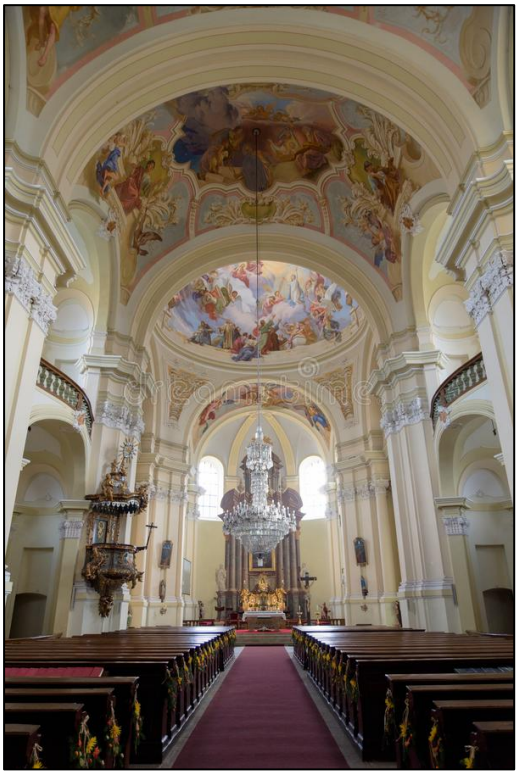

Figure 6 Interior of All Saints Church - Hermankovice

3.6 Saint Anna Church, Vižňov

The main wooden church in Vižnov before the Thirty Years ' War was a parish church, then it was a branch of Vernérovice. The construction of the current church of St. Anna began in 1724 and was completed four years later. The architectural design has been given by Kilian Ignaz Dientzenhofer. The body of the church has a profound, oval projection of the floor, with the middle sections of the side walls mildly curved. Two similar sections of the building with round corners are attached to the smaller side. It has a little chancel on the west side and a low sanctuary next to it. There is an organ loft on the east side with two spiral staircases and a prismatic tower is installed beside it. The builder of the tower was Johann Heinrich Opitz from Ruprechtice.

Figure 7 Interior of St. Anna Church, Viznov

The hipped roof was originally covered with shingles. In 1903, it was replaced with slates and in the1990s, with metal, red-painted profiles. Today, there is almost nothing left from the original equipment in the church because all valuable movables were deposited in the collection storage rooms after the baroque painting had been stolen from the church in 1990. [7]

Figure 8 St. Anna Church, Viznov

This page is left blank on purpose.

4. THEORY

The chapter aims to briefly introduce the issue of the presence and movement of water in a porous environment along with the characteristics.

4.1 Porous Media

Materials have either a two phases or three phases composition. A two phases composition is having a material composed of solid particles and pore spaces. A dry material has solid particles and pore air and a fully saturated material has solid particles and pore water. A partially saturated material has three phases, solid particles, pore water and pore air. Materials such as masonry, are considered porous and have the same composition solid materials/particles and pore spaces. [8] [9]

4.1.1 Porous Media Characteristics

Generally, the soil is a porous material consisting of solid mineral particles with interconnected pores. Like most building materials, including masonry is porous, formed by a solid skeleton and pores. The overall volume of pores and their size, shape and interconnection are of great importance for the properties of the materials.

Porosity

Porosity indicates the mutual ratio of the volume of pores, i.e. the part of the soil formed by free space, to the total volume of the porous substance.

The pore volume ratio to the total pore sample volume is expressed by porosity (*n*)

$$n = \frac{V_p}{V} \qquad \textbf{Eq. 1}$$

Where V_p is the volume of the pore and V is the total volume of the sample.

Bulk Density

This quantity specifies the mass of the solid sample in the overall volume of the soil sample, where the degree of soil compaction is often taken into account. The value is determined by the intact soil sample. (ρ_d)

$$\rho_d = \frac{m_s}{V} \qquad \textbf{Eq. 2}$$

The bulk density values depend on the soil texture , structure and organic matter content. Which vary from 0.5 g/cm^3 to soils with a high organic matter content to 2.65 g/cm^3. Most soils are between 1.2 g/cm^3 and 1.8 g/cm^3.

Particle Density

The particle density or specific gravity only expresses the bulk density of the dry phase. This is therefore expressed as the weight ratio of the solid phase to the volume of the solid phase. It does not depend on the soil texture and can be determined by a broken sample. *(ρ_s)*

$$\rho_s = \frac{m_s}{V_s} \qquad \textbf{Eq. 3}$$

In general, the density values are approximately 2.65 g/cm^3, but if the soil contains a high proportion of organic matter, the value can be as small as 1.5 g/cm^3.

4.1.2Water in Porous Medium

Volumetric Water Content & Gravimetric Water Content

The quantity of liquid (water) in the porous material indicates humidity. It is possible to assess either the volumetric water content (θ)

$$\theta = \frac{V_w}{V} \qquad \textbf{Eq. 4}$$

Where V_w is the volume of water and V the total volume.

Expressing the ratio between the volume of water and the total amount of soil or the mass of moisture (w)

$$w = \frac{m_w}{m_z} \qquad \textbf{Eq. 5}$$

Where m_w the weight of the water and m_z the weight of the solid phase. When all the pores of the material are filled with water, the volumetric humidity is equal to the porosity, and then it is a saturated environment. If only part of the total pore volume is filled with water, it is an unsaturated environment.

Degree of Saturation

The degree of saturation is the ratio of the volume of water to the volume of void (S_r)

$$S_r = \frac{V_w}{V_v} \qquad \textbf{Eq. 6}$$

The degree of saturation may vary from zero for completely dry soil to 1 for completely saturated soil.

4.2 Moisture Potential

Soil-moisture potential refers to this relative level of the potential energy contained in the soil water. Soil moisture potential is an expression or indicator of the potential energy contained in soil water relative to that of water in a standard reference state. Soil water is subject to the work-energy principle, which states that the work done by an object is equal to change in its energy status. If positive work is done on soil water, soil water's potential (energy) status increases equal to the work w done on it. If negative work w is done on soil water, the soil-moisture potential (energy) decreases by an amount w. [10]

4.3 Retention Curve

The retention curve, which describes the relationship between moisture potential and volumetric soil moisture, is an important hydraulic characteristic of the porous medium and thus shows the capacity of the soil to retain the amount of water under various pressure conditions.

When a dry porous medium is moistened, the pores are slowly filled from the smallest to the largest. When drained, on the other hand, the larger pores are first filled, then the smaller ones. For both processes, each soil moisture value refers to a certain capillary pressure deriving from the varying curvature of capillary menisci in relation to various capillary widths or sizes of water-filled pores. The relationship between soil moisture and capillary pressure is determined by the line of retention.

The typical curve of retention for such soil types is shown in Figure 9. The differences along the curve for each material are caused by the dependence of soil structure, grain size and mineral composition, physico-chemical characteristics and humus content. [11]

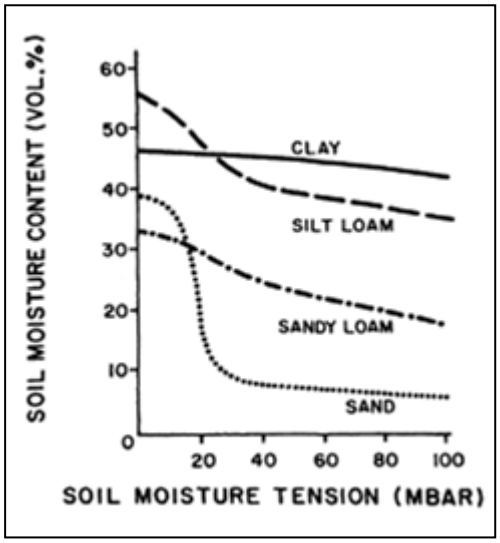

Figure 9 Example retention curves showing the relation between moisture content and soil moisture tension for soils of different texture [11]

4.4 Hydraulic Conductivity

This characteristic expresses the ability of the porous medium to conduct water, has a dimensional velocity which relies on the characteristics of the porous medium as well as the flow properties of the liquid. Hydraulic conductivity is largely influenced by the properties of the fluid and its viscosity density. There is a distinction made between saturated and unsaturated hydraulic conductivity. [11]

The saturated hydraulic conductivity is known as K_s. The calculation is carried out either in the laboratory at undisturbed, completely saturated sample, in constant or variable slope of the hydraulic

heads. The so-called double-ring infiltration experiment is then determined in the field by the two-cylinder method, where the full water saturation of the soil must again be assured. The saturated hydraulic conductivity is calculated on the basis of Darcy 's equation. Hydraulic gradient and flow volume. Saturated hydraulic conductivity values for clay soils range from 10^{-12} to 10^{-6}, sandy soils range from 10^{-7} to 10^{-3} m/s.

The value of unsaturated hydraulic conductivity marked *K(θ)* depends on soil moisture shown in Figure 10.

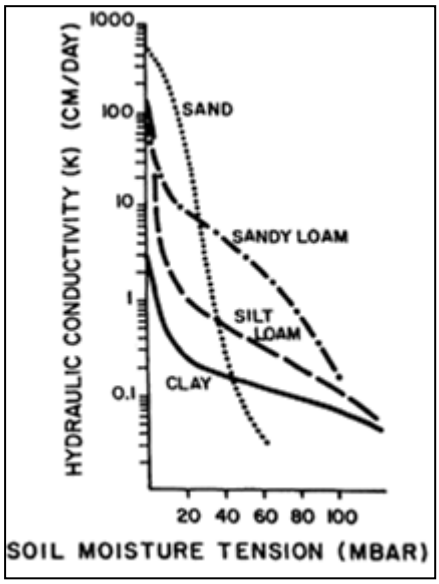

Figure 10 Example characteristic curves showing the relation between hydraulic conductivity and soil moisture tension [11]

Unsaturated hydraulic conductivity can be measured on site using a tension infiltrometer or calculated. Considering the distribution of the known pore size from the retention curve and the Laplace equation and the equation defining the flow in each capillary.
Unsaturated hydraulic conductivity can be estimated on the basis of the following formula:

$$K'(\theta) = K_r(\theta)K_s \qquad \textbf{Eq. 7}$$

Where *K´(θ)* is an approximation of unsaturated hydraulic conductivity, K_r is the relative value of hydraulic conductivity and K_S is the saturated hydraulic conductivity. The relative values for hydraulic conductivity are obtained from the integration of the retention curve. There are many relationships for the integration of the retention curve, the best known of which is the method of the author Mualem in 1976 [12], which improved the relative estimation of hydraulic conductivity by integrating the influence of relative tortuosity (diffusion and flow of fluid in a porous medium):

$$K_r(\theta) = (\frac{\theta}{\theta_S})^{\frac{1}{2}} = \left(\frac{\int_0^{\theta}\frac{d\theta}{h_c}}{\int_0^{\theta_S}\frac{d\theta}{h_c}}\right)^2 \qquad \textbf{Eq. 8}$$

where $K_r(\theta)$ is the relative hydraulic conductivity, θ humidity, θ_s saturated humidity and h_c capillary pressure head.

4.5 Water Flow in Porous Medium

Movement of water in a porous environment may be tracked and represented at different rates. The most comprehensive and detailed description shall be at the molecular level. The individual pores are described by the determination of the movement at the microscopic level. The actual phase is replaced by a continuum that fully fills a portion of the space. It is necessary, however, to tackle the problem of flow through a porous medium at a macroscopic level, as the microscopic scale is too detailed. Through this method, pore space is continually filled with fictitious macro-continuities that interact with each other in an overlapping manner. It is not necessary to describe exactly the limits of the different micro-continents, making the calculation easier. [10] [9]

The capillary bundle concept provides the simplest explanation of the movement of water through the porous system. This concept implies that the soil matrix is made up of thin, straight capillary tubes of uniform size and shape. The capillary bundle concept may contain some of the non-uniformities of natural soils by considering a capillary structure that is neither parallel nor equal in size and shape.

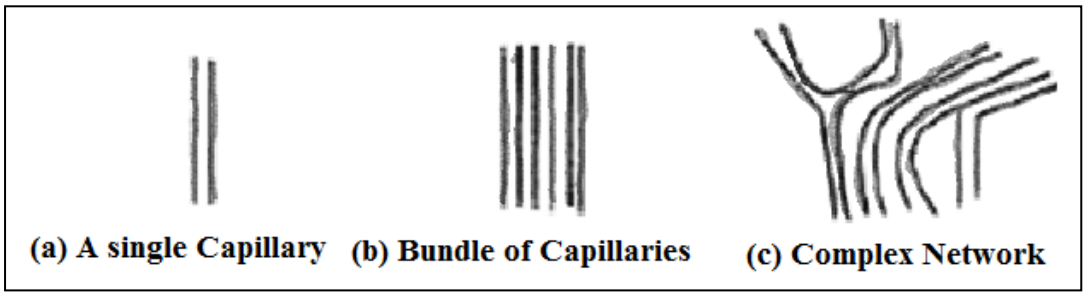

Figure 11 Capillary Bundle Concept [11]

In fact, a soil matrix may be made up of pores with variable diameter and/or dead-end pores. The microscopic analysis of the single pore flow inside the soil matrix is difficult to describe using the capillary bundle concept. However, the capillary bundle concept is useful and important for the macroscopic description of the soil matrix, see Figure 11.

4.5.1Water Flow in a Saturated Environment

This type of flow exists in open surface aquifers, where the upper bound is a saturated zone with a free groundwater level and the lower bound is an impermeable or semi-permeable layer. And in confined aquifers, where the lower and upper limits are formed by an impermeable and semi-permeable layer.

Darcy's law

Henry Darcy, by examining the flow of water through a given volume of saturated porous medium, evaluated its direct ratio to the hydrostatic pressure difference at the beginning and end of the resolved zone *ΔH*, to the cross-section of aquifer *A*, and indirectly to the length profile of *L*.

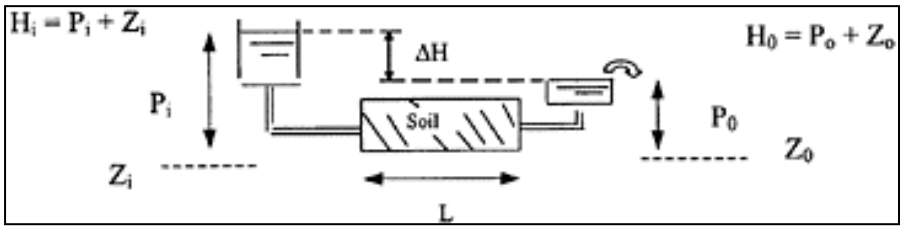

Figure 12 Flow across the cylindrical system [11]

The hydraulic gradient (*ΔH*) across the soil matrix is given as follows(Figure 12):

$$\Delta H = \frac{H_i - H_0}{L} \qquad \textbf{Eq. 9}$$

where H_i and H_0 are the hydraulic head maintained at inlet and outlet of the soil column, respectively, and *L* is the length of flow or soil column.

The volumetric flow rate is:

$$Q = K_s \frac{A * \Delta H}{L} \qquad \textbf{Eq. 10}$$

with K_s the saturated hydraulic conductivity of the soil matrix.

Thus *q* is the flow per unit cross sectional area per unit time, and is called flux density is:

$$q = K_S \frac{\Delta H}{L} \qquad \textbf{Eq. 11}$$

4.5.2Water Flow in an Unsaturated Environment

An environment is considered unsaturated when some of the pores are filled with water and the remaining pores with air. Similar principles apply to the flow of water in an unsaturated material as to saturated flow, but the process is more complicated by the fact that the part of the pores filled with air can be saturated with water during the flow, or conversely the pores can be drained.

Darcy-Buckingham law

This is a change to Darcy 's law for use in an unsaturated environment. Flow density here does not rely on saturated hydraulic conductivity, but on unsaturated hydraulic conductivity, the value of which varies depending on soil moisture. The generalized formula for volume flow is therefore as follows:

$$q = K(\theta) \frac{\Delta H}{L} \qquad \textbf{Eq. 12}$$

Continuity equation

The continuity equation combines the rate of change in soil matrix moisture content with changes in incoming and outgoing flow through the soil matrix. Continuity equation indicates that the rate of change of input and output flux is equal to the rate of change of storage in the soil matrix.

By applying the law of conservation of mass, the continuity equation in a three dimensional environment (Figure 13) can be expressed in the form:

$$\frac{\partial \theta}{\partial \mathrm{t}} = -\left(\frac{\partial q_x}{\partial x} + \frac{\partial q_y}{\partial y} + \frac{\partial q_z}{\partial z}\right) \qquad \textbf{Eq. 13}$$

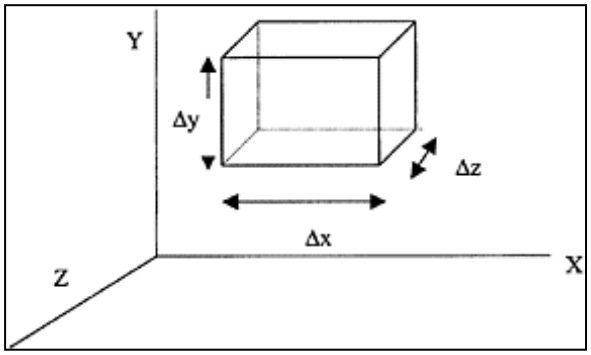

Figure 13 Three dimensional section of soil matrix [11]

with q_x, q_y, q_z the volumetric fluxes in all the three directions.

Richards equation

Richards equation is obtained by the substitution of Darcy-Buckingham law into the continuity equation

$$\frac{\partial \theta}{\partial \mathrm{t}} = \frac{\partial}{\partial x}\left(K(\theta)\frac{\partial H}{\partial x}\right) + \frac{\partial}{\partial y}\left(K(\theta)\frac{\partial H}{\partial y}\right) + \frac{\partial}{\partial z}\left(K(\theta)\frac{\partial H}{\partial z}\right) \qquad \textbf{Eq. 14}$$

where $K(\theta)$ is the coefficient of unsaturated hydraulic conductivity, $\frac{\partial H}{\partial x}$, $\frac{\partial H}{\partial y}$, $\frac{\partial H}{\partial z}$ are the hydraulic gradients in the appropriate directions; and $\frac{\partial \theta}{\partial \mathrm{t}}$ is the change in water contant over time.

By resolving the Richards equation, we obtain information on the spatial-temporal development of all considered state variables (water content, pressure head, flux) within the selected flow region. The equation defines the flow in a real porous medium under the following simplified conditions: the medium is stationary and non-deformable, the air pressure in the pores is constant and the air pressure in the pores is non-deformable and the circulating water is uncompressible.

This page is left blank on purpose.

5. LITERATURE REVIEW

Many studies concerned with the moisture of buildings, describes moisture as a significant or one of the key issues affecting heritage buildings. They reflect it as the originator or, at the very least, a source to all decomposition processes for building materials. We can also consider a variety of studies evaluating the state of specific historic structures, including the transfer of moisture, soluble salts and other problematic effects on building structures.[13] [14]

5.1 Sources of Moisture in Historical Structures

In order to address the problem of the transport of moisture to the masonry material, the origin of water entering the structure should be considered. Studies can be noticed that, in addition to the movement of moisture already existing in the material, there is an attempt to incorporate moisture sources (and other influences) entering the building external sources [15] [16]. But they still overlook the subsoil as a source.

Exchange of air, heat and moisture between the interior and the exterior of a building was modeled in this study [15]. In the model, the construction of the walls and ceilings of the building, the indoor environment and then the local outdoor conditions act as key factors in the exchange of heat and moisture. The interior climate of the building is largely due to indoor temperature and relative humidity. Outdoor environments include rain, wind blowing on the building walls, and sunlight. The transfer of heat and moisture from the ground wasn't included at all. Thus, the study found that the indoor environment can accurately predict the indoor humidity, energy consumption and durability of a building.
The study [16] also focuses on the environmental impact on buildings and the transmission of temperature and humidity through a buildings' envelope and the interaction with the building's indoor atmosphere. Again, only the air properties that impact the building material, both from the outside and from the inside, are considered, and the effect of the interaction with the subsoil is neglected in this work. The results show that not accounting for hygrothermal effects in modeling will result in overestimation of energy costs for hot and humid climate situations.

The inclusion of a building subsoil in the model is described, in a study by [17]. The problem of heat and moisture transfer is described as the interaction of three areas: the soil, the building envelope and the air inside the building. In addition to the models without subsoil influence, a heat transfer solution from the ground to the floor has also been developed. Heat transport is solved by equations based on Philip and De Vries' theory (1957) of the transport of heat and water through porous media, which derives leading equations using the finite volume and three-dimensional model methods to explain the transmission of heat and moisture by unsaturated, moist soil and bottom construction, and the effects of room temperature and relative humidity. The results of the study are, a higher energy consumption

is expected when an air conditioning system is used due to the augmentation of building latent loads and the absence of solar radiation during the rain period cause room temperature reduction.

In summary, it can be said that the main sources of moisture in building structures, and therefore inside buildings, can first be described as capillary rise of soil water and storing and transporting the associated soluble salts. In addition, precipitation, whether or not influenced by wind, as well as condensed moisture in indoor and outdoor air.

5.2 Risks of Moisture in Historical Structures

The study [18] addresses the side effects caused by moisture and the explanation of indicators suggesting damage to masonry. Masonry damage was classified into four groups according to how moisture leads to material degradation. The first of the four groups applies to damage done by direct moisture, further degradation by the action of moisture as a vector, the third to damage occurring in a wet environment, and the fourth to damage caused by the appearance of moisture indoors.
The direct influence of increased moisture involves worse thermal insulation properties, lower mechanical strength and changes in the volume of structures. The mechanical strength of the material decreases with increasing humidity and the stability of the structure becomes at risk as the critical humidity of the masonry is reached.Thermal conductivity of masonry rises with increasing humidity, since the coefficient of thermal conductivity of water is 25 times greater than the air that occupies the masonry pores in dry conditions.Wet masonry therefore increases the heat loss from the building, so that when masonry moisture increases by 1 per cent, the heat flow increases by 3-5 per cent. Volume changes refer to the swelling and shrinking of porous materials by the structures. Water in the pores exerts pressure on the solid phase and thus changes in volume, which can eventually lead to material defects.
Damage caused by the action of moisture as a vector is due to the gradient of the water content in the pores of the various parts of the masonry. It is possible to distinguish between two types of such damage. One is frost damage, the other is salt crystallization. Frost damage is associated with a change in water volume when it is frozen. Freezing cycles in micropores are extremely harmful because there is not enough room to expand and therefore ice disrupts the solid phase of the masonry. Damage caused by salt crystallization is caused by the transport of these dissolved salts by water during capillary rise and subsequent deposition. Throughout deposition, recrystallization occurs, which may lead to material surface loss, e.g. in the form of peeling.[18]

Damage resulting in a wet environment can be separated into biological damage and corrosion damage. Biological damage or biodegradation is caused by different types of organisms, the presence of which is determined by sufficient source of water, a suitable temperature for organisms and exposure to light. These include bacteria , fungi, algae, and lichens. These organisms are possibly toxic to the population since they can trigger allergies or disease. Corrosion causes different forms of

damage, ranging from corrosion of the façades to the complete loss of some parts of the structure. This harm is caused by the cracking of the material leading to the development of a corroded metal layer, which increases the volume of the metal components. Corrosion occurs when the metal reaches the temperature of the dew point. Water vapor then liquefies on the surface of the metal to create a liquid coating that causes the metal to oxidize. [18]

Damage done by indoor humidity influences the comfort of the occupants in terms of temperature and air quality. In the case of temperature, living comfort is defined by means of a static or adaptive approach. The static model uses PMV (Predicted Man Vote) and PPD (Predicted Percentage Dissatisfied) indicators that quantify the atmospheric temperature of the inhabitants as a function of ambient temperature , relative humidity, clothing quantity and air flow. The pragmatic approach also takes into account human activity in this environment and attempts to maintain suitable conditions. Air quality is assessed against pollution indicators such as bacteria , viruses, volatile organic compounds, dust mites and fungi. The quantity of these pollutants depends mainly on the presence of water, in this case in the form of water vapor, and therefore on the relative humidity of the air. The optimum level of relative humidity for healthy ambient air quality is 40 to 60 per cent. [18]

5.3 Corrective Measures and Moisture Removal

[13] and [19] discussed remedial measures aimed at reducing the problem of rising damp in the masonry of historic buildings, particularly in terms of technologies for their removal. The corrective measures are discussed below with their advantages and disadvantages

The earliest example of remediation is the construction of a near surface drainage system near the building. The idea is to reduce the level of the groundwater table to the appropriate height, which works consistently with the system. However, this method does not prohibit capillary water from rising and it is important to consider various efficiencies influenced by soil properties. Another downside is the relatively large size of the system and the setup cannot be used, for example, when other structures are near to the problem being addressed. [13] [19]

One of the other methods used to retain moisture from rising into masonry is to insert watertight barriers in horizontal layers directly into the structure, thus preventing the rise of water. Nonetheless, issues also occur during execution, as it is very difficult, if not impossible, to apply this method to very thick walls, as is generally the case in churches. Thereafter, vibrations are triggered during installation, and can endanger the structure. It has also been shown that this measure decreases the shear resistance of the masonry and thus endangers the stability of the structure during earthquakes. In conclusion, the fundamental goal of the implementation of this method, which is rather inefficient below ground level, is not achieved and the effects are not ideal even on the soil. There are cases

where the volume of water in the masonry under the barrier is almost completely saturated, which may cause significant damage to the masonry due to decreased mechanical resistance. [13] [19]

Another method is to create a chemical barrier by using hydrophobic chemicals that, unlike the previous method, stop the flow of water through masonry on a chemical rather than a physical basis. Chemicals are added by grouting directly into the foundation of the structure. The drawback of this method is the need for the chemical to access all the pores of the masonry. If this is not the case, the transport of water through the masonry will not be interrupted. For this reason, a large number of studies have been carried out which show that the results of the efficiency of the chemical barrier as a corrective measure have not yet been fully concluded. This depends mostly on the following factors: the chemical in use, the injection pressure, the masonry material, the existence of cracks in the masonry and the degree of saturation of the masonry. [13] [19]

Measures are also based on the concept of increasing evaporation, which decreases the water content of masonry. Which include the so-called Knapen tubes, the foundation ventilation system, the regenerative plaster and the thermal method. [13]

Knapen pipes or air drainage siphons operate on the principle of a higher mass of moist air unlike dry air. Tubes fabricated of fired clay or perforated plastic are installed obliquely directly in the masonry and wrapped with porous mortar. Due to the orientation of the tubes, which are led obliquely outward from the inside of the wall, the heavier humid air must be brought down to the outer edge of the wall, where evaporation occurs, and the dry air inward. Unfortunately, this method has proved unsatisfactory and even causes an increase in masonry moisture under certain circumstances, such as in unheated rooms or the lack of direct sunlight on the outer surface of the wall. [13] [19]

In the positive side, the ventilation system for masonry foundations is a successful strategy based on increased evaporation. Ventilation is provided by ventilation ducts that lead to shafts opening above the surface of the surrounding land. Such ducts are mounted on the outside of the masonry and on the inside under the floors in the shape of porous tubes. The system reduces the humidity of the masonry as compared to the condition without intervention, in both laboratory and in the field. Of course, the efficiency depends on the masonry material and its size, but the system is usually considered to be efficient. However, research is still needed, in particular on the effects of crystallization on the ventilation system. [13]

The renovation of plasters promotes the evaporation of the outer surface of the building walls and at the same time reduces the damage caused by the crystallization of soluble salts. They are very porous materials that accelerate the transport of water vapor and significantly reduce capillary rise due to their large pores. Attenuation of the damage caused by soluble salts is then achieved in some types

of coatings by depositing the salts in their pores, in others by sending the salts to the outer surface where they crystallize without causing damage. In practice, however, the action of regenerative plasters is sadly not always useful, mostly due to the material 's lifetime. Efficacy often relies very much on the characteristics of the environment, due to which the type of plaster will be selected accordingly, which is sometimes ignored, and the system does not necessarily attain optimal efficiency. [13]

Finally, also there is a method based on the principle of electrokinetics that uses the appearance of an electrical bilayer on the surface of the capillaries in porous materials. This method , called active electro-osmosis, is based on the principle of implementing an external electrical field into the soil-masonry system , which causes the transfer of the particles inside the water. The development of an electrical field is accomplished by the application of electrical current by means of electrodes mounted in the masonry and in the soil. By producing an electrical current, the electrons move between the masonry that is the anode and the ground that becomes the cathode of this system, which in effect allows the masonry to dry out. This study was developed on a historic building in the city of Kronstadt, which has resulted in a significant reduction in humidity. A lot of attention is then applied to the location of the anode. It must not be situated above the maximum capillary rise or else, the system is not functional. [13]

5.4 Moisture Measurement Methods and their Applications

Some of the studies concerned with the methodology for measuring moisture in masonry is discussed in the paper [20] and its benefit would be that it can be used for periodic measurements over extended periods of time. The study also summarizes and explains the major types of methods used for determining moisture content in masonry.

Indirect methods refer to infrared thermography, which identifies wet areas from dry areas by specific temperatures and can be used to examine an entire building, but does not allow for the real possibility of quantitative measurement and after all, it is possible to evaluate only the relatively thin surfaces, which are also the most influenced by ambient conditions. So it may vary greatly from the internal layers of the material. In addition, measurement of the electrical resistance of a porous material (resistance method) is stated, which reduces water content and is simple and inexpensive to measure. When measuring the wave attenuation caused by moisture using a microwave technique, the impact of the salt concentration on the measurement can be decreased by using a very high frequency. Radar tests may be used to examine the speed of propagation of electromagnetic waves through humid masonry. However, the last two methods do not produce quantitative results without extensive calibration, which requires sampling of the object under examination and installation of the sensors on site. Neutron dispersion and nuclear magnetic resonance methods are very difficult to conduct, the former because of safety criteria and the latter because of the size of the instruments needed. The last

indirect method described is the relative measurement of air humidity under equilibrium conditions, either in a closed cavity within the material or in a container in which a sample of material is inserted. In this approach, nevertheless, it is necessary to measure the temperature at the very same moment as the results depend on it and, at the same time, to assess the quantitative relationship between the measured air humidity and the required material humidity for each particular instance. [20]

Among the direct methods for the quantitative determination of moisture, the calcium carbide method is used. It can be done in the field, but it can lead to loss of moisture, which leads to an underestimated percentage of units. Error related to the collection and handling of samples may also occur in the gravimetric method often used. This can also be achieved in the laboratory and field using portable thermal scales. Nonetheless, working with this method is not simple, and the risk of measurement errors increases further.

On the basis of an analysis of the known methods, the authors decides the requirements for the highest possible accuracy and informational measurement capabilities and shall derive their method. The first criterion is the accuracy and reliability of the data obtained, which, according to the authors, cannot be accomplished gravimetrically. The second requirement is the collection and careful storage of appropriate representative samples within the material for laboratory measurements. It is proposed to measure at many locations at various heights above the ground up to the height of the so-called equilibrium line, but at the same depth in the matter. As a condition for determining the relevant data , the authors place the probability of repeated long-term measurements in the same brick (material). This is essential because of the large difference in the microstructure of these units (bricks), which is important in historical buildings due to poor craftsmanship, and then in natural building materials. The last condition is to prevent the moisture conditions in the masonry from being affected by the measurement itself, which is why the authors consider it necessary to close the sampling openings carefully and thus avoid drying through these cavities. [20]

To verify the method, two laboratory models made up of bricks currently in production have been developed. Permanent sampling points were formed by drilling cavities of 9 cm deep and 1.5 cm in diameter. The drilled brick pieces were re-inserted in the cavities. The cavities were then sealed by rubber stoppers and plasticine. The models remained in a 2 cm layer of water until a stable state was reached, which happened after about two months and was determined by repetitive weighing of the samples stored in the cavities. Then, the moisture content of all model components was determined after drying and comparison of the weights, and the temperature and relative humidity of the air inside the cavities, the pore size distribution in the samples and the soluble salt content were measured.

Model 1 material had a lower porosity (39.1%) than Model 2 (46.1%). It explains the slightly higher measured moisture levels for the second model (29.39 per cent in the lower part to 24.33 per cent in

the upper part) than for the first model (20.78 per cent to 15.67 per cent). The measured moisture content of the brick powder formed during the drilling process was significantly higher (about 30 to 45 per cent) than that of the preserved pieces, even relatively small ones (0.2 to 0.7 g) inserted in the cavities, which is attributed to the higher specific surface area and excludes the use of the powder as a representative sample. On the other hand, the low variance of the measured values for fragments of various sizes and for the entire (pierced) brick indicates a strong representation of these samples. [20]

On the basis of experience, the authors advise that fragments should only be removed and measured from the cavities after the equilibrium with the surrounding material has been achieved, i.e. at least one month after the fragment has been inserted. It is also recommended that sampling points be established at a minimum of three heights: 20 to 30 cm above the ground, the second in the wet zone and the third in the dry zone well above moisture pick-up line. For historic buildings, openings with a diameter of 15-20 mm and a depth of 15-20 cm are recommended. [20]

The study [13], by improving the previous method of measurement, mainly examined the importance of the mortar layers between the different masonry components on the capillary rise of water and salt transport and the related electrokinetic effects in masonry as a whole. The research was carried out in the laboratory on three units composed of bricks bonded by different types of binders, namely hydraulic lime mortar, cement mortar and lime mortar with brick dust. After stabilization, the moisture and salt content of the samples collected in the laboratory and field was measured using samples obtained using a permanent sampling point method and the electrical potential were measured using electrodes inserted into the material.

In the case of laboratory samples, the humidity increased at the lowest in the case of a cement mortar sample, slightly higher in the case of a lime mortar, and significantly higher in the case of a brick dust mortar where it almost reached the top of the sample. The results are related to the porosity, which is highest in bricks, slightly lower in the mortar with brick dust and significantly lower in lime and even more so in cement mortar, but also to the pore diameter, which has a similar evolution in the materials studied and affects not only the total amount of water absorbed, but also the rate of increase. The very existence of interfaces between materials, where pore systems do not connect, and imperfect contact between elements can also contribute to a significant reduction of rising moisture through mortar layers. During measurements in a historic building, moisture values ranging from 15-20 per cent on the floor surface to 7-8 per cent at 2 meters above ground level were found at indoor measurement points; outside, soil moisture reached approximately 12 per cent, decreased rapidly at height and was almost zero at 2 meters, all of which were assumed to be due to increased evaporation. However, over the course of the year, the values have not changed significantly. [13]

[21] study examines the movement of humidity in the historic masonry of the Cathedral of Lecce in southern Italy. The building, carefully divided by the authors into an underground crypt and the upper part of the cathedral, is made of local material-fine-grained porous limestone. The study aims to identify the basic characteristics of moisture activity in masonry without the use of complex numerical methods involving extensive data and measurements. The flow of water through the monolithic blocks and the overall masonry structure takes into consideration the usage of the "sharp front" theory, which substitutes the gradual transition of the wet and dry parts of the material with a clear boundary. In the case of complex geometry and structures composed of several materials, the model should be well usable. The study derives and applies the relationship for the direct and indirect measurement of water evaporation from a material whose input parameters are available in meteorological records (temperature, relative humidity , wind speed and solar radiation).

It was found that the building material could absorb water quickly and dry out at the same time. On the basis of the measurements, the author considers that the contribution of the foundation soil water to the masonry is significant only during the rainy months, while it is negligible during the summer months. However, it should be noted that the object studied is located in the Mediterranean climate with hot and dry summers and mild winters rich in precipitation. Among other sources of humidity, the author mentions infiltrations, washing water, leaking pipes and sewers. The influence of soil moisture was only noticed by the author in the building in the lower crypt, which "protects" the upper church against it. [21]

5.5 Sandstone Characteristics

[22] research deals with the combined transport and storage of water and salts in sandstone Mšenská, a fine-grained calcite-clay material collected from quarry Mšenélázně in northwestern Bohemia. The research uses a model of diffusion-addition which takes into account the effect of water flow on salt transport and the effect of bound salts in the pore walls. It considers moisture conductivity and water vapor diffusion coefficient as parameters of water movement and takes the isothermic sorption and water retention curve as parameters of moisture storage-properties that can be determined by samples taken directly from the original object or quarry in a standard laboratory way, as is the case in case studies.

A bulk density of 1850-1930 kg/m^3 and a porosity of 26.25-29.67 per cent was found from the material's basic characteristics. By assessing the retention curve, it was observed that the moisture is maintained similar to saturated moisture at a pressure height of up to 3 bar, and by far the most important decrease in moisture was recorded within a pressure range of 3 to 5 bar (from a moisture value of approx. 0.16 to approx. 0.01). The authors estimate most pore sizes to range between 0.5 and 0.3 μm based on this discovery.

The authors identified as the most important of the characteristics recognized a very rapid capacity for transportation of water, which has therefore a double impact in terms of property damage-as it allows for fast transfer of water from a wet area, it also allows easy transportation of water from the underlying soil to the masonry. Also found was easy permeability of water vapor, which the authors consider to be a beneficial property due to the likelihood of evaporation, i.e. indoor condensation prevention.

Nevertheless, according to the researchers, the type of material used was used mostly for non-load - bearing structures and decorative works (ornaments, sculptures), whereas for load-bearing structures, more coarse-grained siliceous sandstone was used.

Also, the study [23] determined experimentaly the hydraulic properties of sandstone (Figure 14). Where 3 samples were collected from the All Saints Church wall in Heřmánkovice. The saturated water content of the sandstone samples was determined gravimetrically based on saturated weight after 7 days of free capillary rise from open bath and dry weight at 105°C to constant weight after drying of the oven. Standard sandbox and pressure extractor methods were used to determine the main drainage branches of the retention curves. The saturated masonry hydraulic conductivity was determined in situ using an infiltrometer.

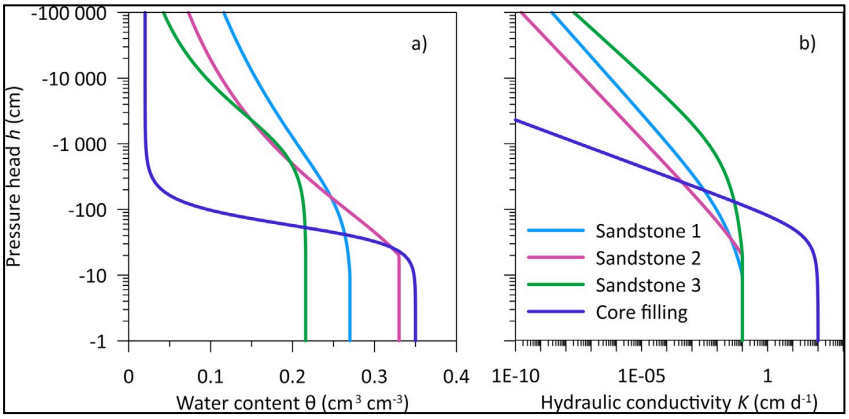

Figure 14 Retention curves (a) and hydraulic conductivity functions (b) for the sandstone samples and the wall core filling. [23]

This page is left blank on purpose.

6. METHODS AND MATERIALS

The work examines the two churches mentioned in Chapter **Error! Reference source not found.**, w hich are the baroque churches from the 18th century, All Saints in Heřmánkovice (Figure 16) and Saint Anna in Vižňov (Figure 15) located in the Broumov region in Czech Republic.

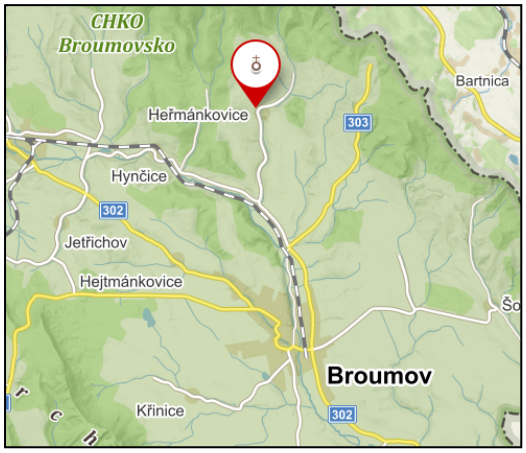

Figure 16 Location of All Saints church in Hermankovice [33]

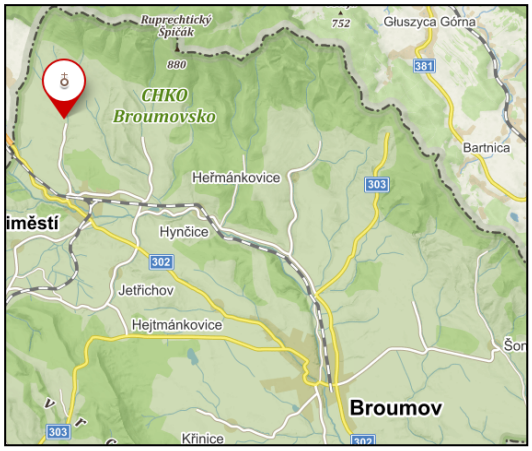

Figure 15 Location of St. Anna church in Viznov [33]

6.1 Site Description

Broumov region is an outcrop of the Hradec Králové region on the northeast, surrounded by Poland on three sides. This area belongs, according to the geomorphological division, to the Broumov Highlands, which are part of the Czech highlands' Krkonoše-Jesenice system. The area of interest is usually defined as a landscape of rugged hills and the highlands of the Hercynica. After the Cretaceous to late Mesozoic period, when the area was flooded by the sea, here remained the most powerful sandstone formation in Bohemia, which was modified by all kinds of weathering in its present form. (Figure 17)

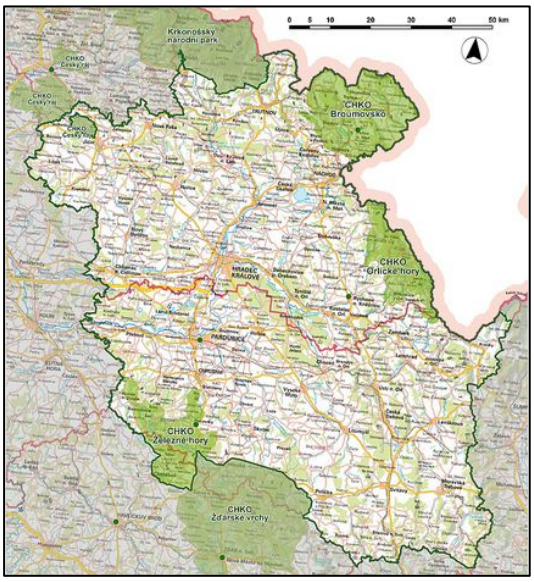

Figure 17 Broumovsko Protected Landscape Area [24]

The entire region is protected under the Broumovsko Protected Landscape Area. The area of Broumov falls within the Odra river basin so water flows into the Baltic Sea from there. [24]

6.2 Climatic Conditions

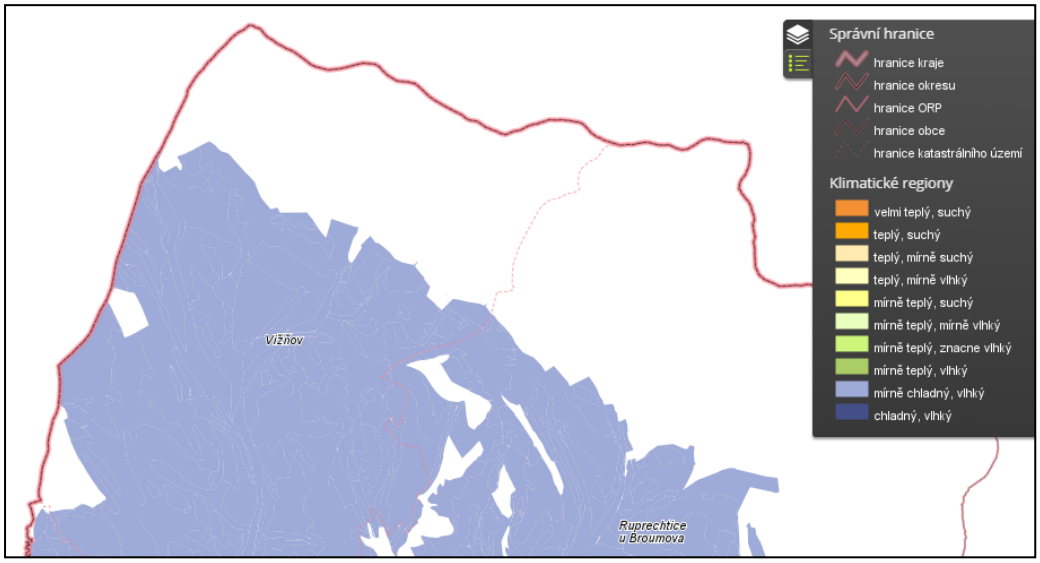

Figure 18 Climatic conditions in Viznov [34]

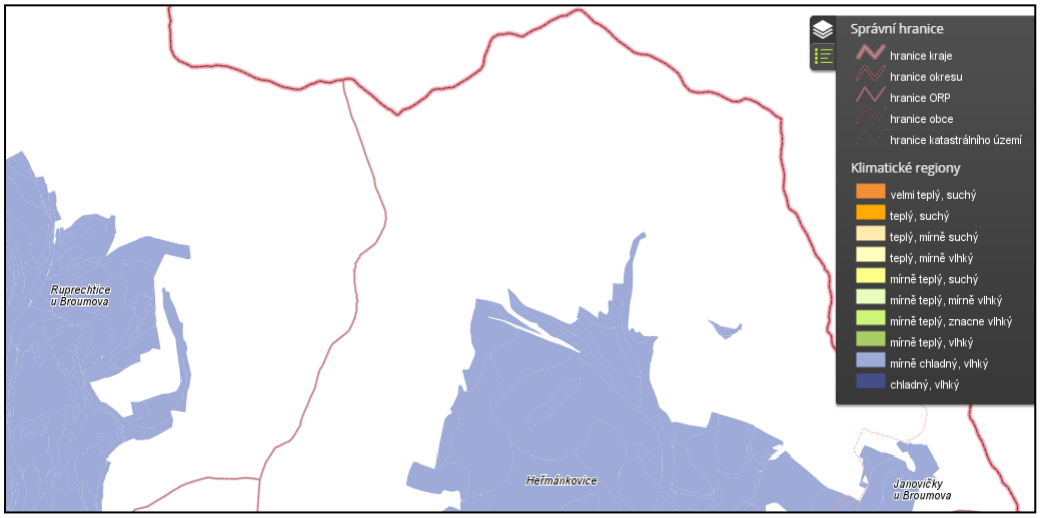

Figure 19 Climatic conditions in Hermankovice [34]

The Broumov region is part of a cold climatic zone within the country, moderately rich in precipitation, with prevailing westerly winds. During the period 2006-2015, the long-term average daily air temperature measured at the Broumov meteorological station is 7.8 ° C, the long-term total annual precipitation measured there for the same period is 620 mm. More specifically The area in which

both churches are situated is in a humid, slightly cold climatic zones (Figure 18) & (Figure 19). The January average temperature ranges from -3 ° C to -4 ° C, the July average temperature is 16 ° C to 17 ° C. The average annual cumulative precipitation ranges from 700 to 800 mm. Snow cover annual averages ranging from 80 to 100 days. [24]

6.3 Geological Conditions

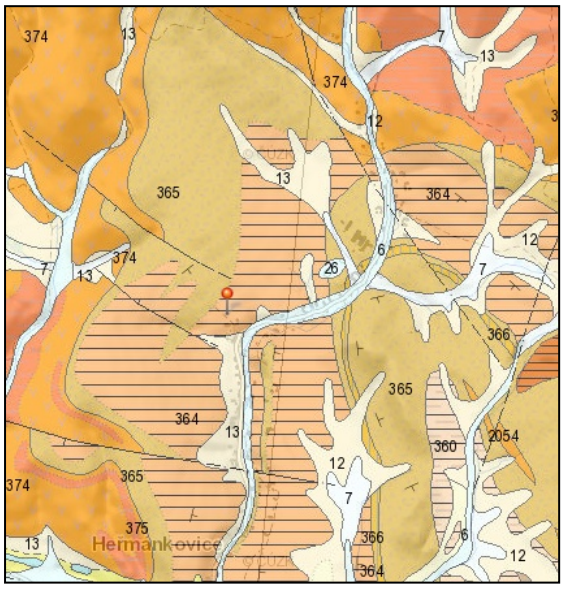

Figure 21 Geological characteristics in Hermankovice [25]

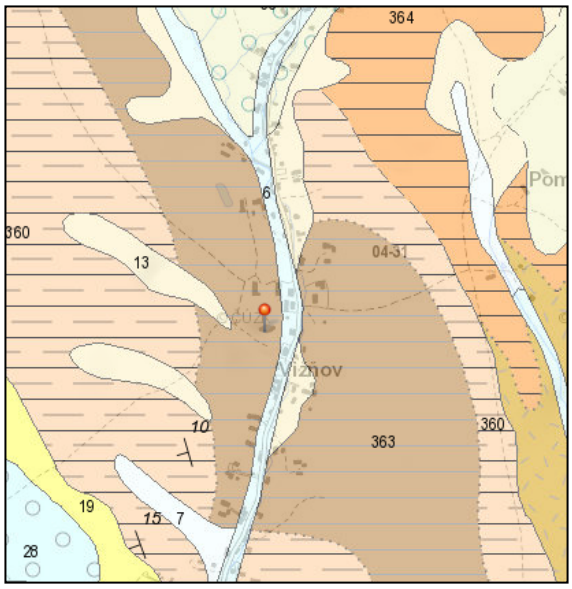

Figure 20 Geological characteristics in Viznov [25]

The church of All Saints stands on a slight hill above the village of Heřmánkovice, at an altitude of approx 460 m above sea level. While the church of St. Anna in Vižňov lies at an altitude of 470 m above sea level. [25]

In Vižňov, the region geologically belongs to the Bohemian Massif, more specifically to the overlying formations and post-variscan magmatites, while the area is known as the Inner Sudeten (Figure 20). The subsoil is composed of consolidated sediments, especially variegated aleuropelites, often calcareous with a silica mixture. For Heřmánkovice, the region geologically is the same as Vižňov and the subsoil is formed from hardened and volcanic sediments, more specifically aleuropelites with a sandstone mixture and volcanodetritic breccias (Figure 21). [25]

6.4 Measurement Methodology

In order to evaluate the water transport in the masonry of the structures, a long-term measurement was carried out on site in both churches buildings and their surroundings. The measurement started in 2016 for the All Saints church and 2017 for the St. Anna church.

6.4.1All Saints Church On-site Monitoring System

In September 2016, CTU researchers installed a system to monitor the moisture and water potential of the masonry and soil at the All Saints Church and its immediate surroundings. Externally, it consists of sensors positioned at two measurement stations north of the church, and, internally, sensors in the north wall's masonry. See Figure 22.

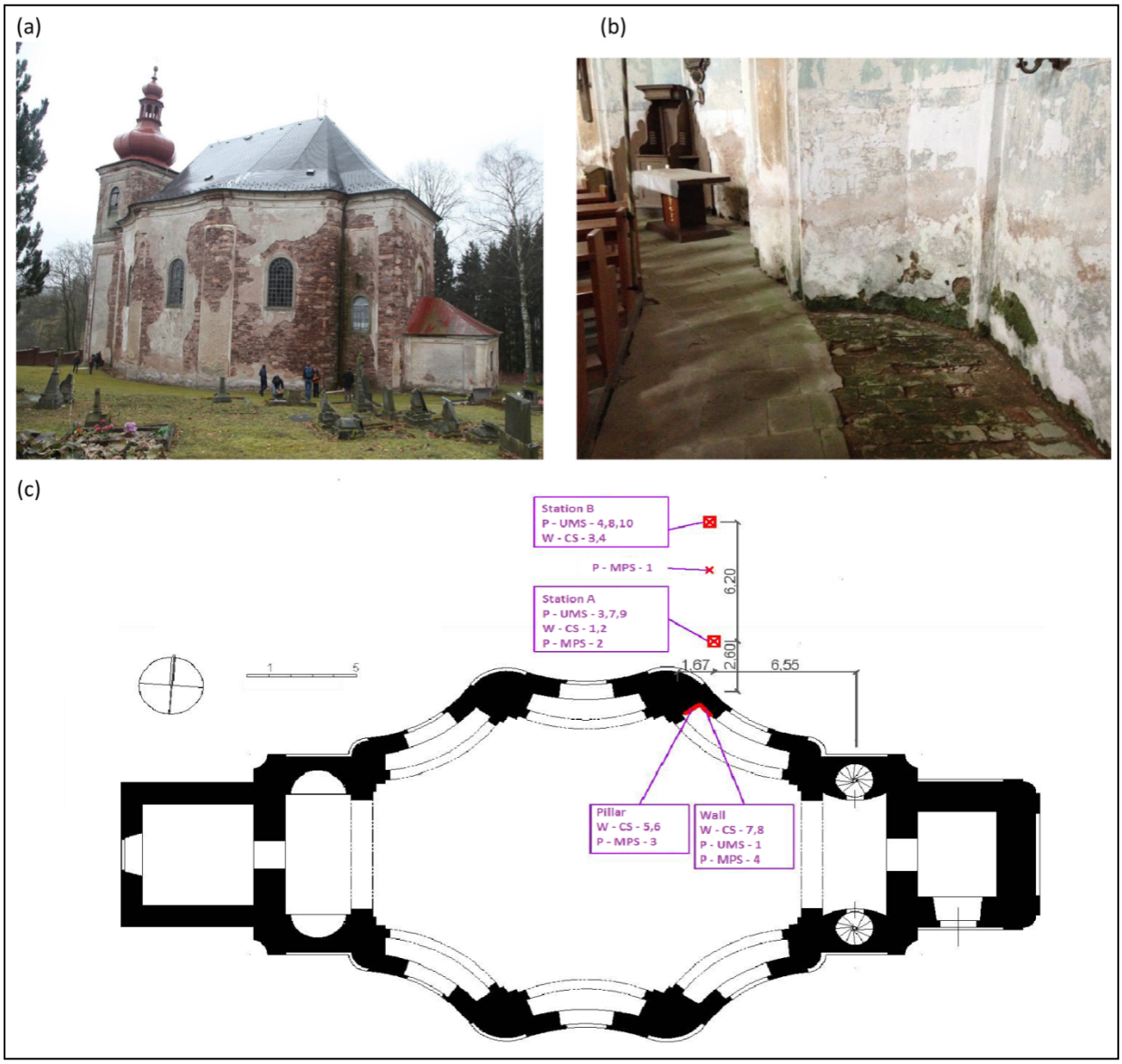

Figure 22 Church of All Saints in Hermánkovice: (a) north facade; (b) church interior; (c) location of the monitoring system. [23]

The church stands in the middle of a cemetery on inclined ground with an average slope of about 13%. The upslope wall, oriented towards the north, is significantly affected by rising damp. The outdoor measuring stations are situated on a slope above the north wall of the church, at distances of approximately 2.6 m and 8.8 m from the building, where the soil surface is 0.39 m and 1.1 m above the ground inside the church. Shafts about 50 cm deep form the measurement stations. For each shaft at various depths are two Campbell scientific CS 650 moisture sensors and three UMS T8 soil tensiometers. There are also MPS-6 (Meter Group, Germany) potential sensors in shaft A, and in between stations A and B at a distance of approximately 6.3 m from the church building, both 10 cm below the ground surface. All sensors of a given type are placed in the ground with the same orientation: moisture sensors and potential sensors against the slope, strain gauges perpendicular to the slope 's direction. Figure 23 indicates the position of the sensors in the shaft, and the depths of the location of their active part are seen in The Campbell Scientific CR 1000, which is the datalogger (control recording unit) is located inside the church in the space of the interior spiral staircase. The measured values of all the sensors described were stored on this unit for the duration of the measurement in a 30 minute time step.

Table 1,Table 2 and Table 3.

Figure 23 Detail of the shaft after installation of sensors

The indoor sensors are located in the north wall of the church, approximately in the extension of a straight line through outdoor measuring stations. They are arranged in two groups, in the parts of the structure that we refer to here as a pillar and wall/niche. The situation of the column and the niche is evident from Figure 24.

Figure 24 Location of sensors in the interior

The Campbell Scientific CR 1000, which is the datalogger (control recording unit) is located inside the church in the space of the interior spiral staircase. The measured values of all the sensors described were stored on this unit for the duration of the measurement in a 30 minute time step.

Table 1 T8 Tensiometer sensor location and depth/height Heřmánkovice

T8	Location	Depth/Height (cm)
1	wall	28
3	Station A	109
4	Station B	129
7	Station A	76
8	Station B	60
9	Station A	41
10	Station B	25

Table 2 CS650 sensor location and depth/height Heřmánkovice

CS650	Location	Depth/Height (cm)
1	Station A	50
2	Station A	29
3	Station B	49
4	Station B	25
5	pillar	10
6	pillar	60
7	wall	10
8	wall	60

Table 3 MPS-6 sensor location and depth/height Heřmánkovice

MPS-6	Location	Depth/Height (cm)
1	between A a B, 3.7 m from A	10
2	Station A	11
3	pillar	45
4	wall	48

6.4.2St. Anna Church On-site Monitoring system

The long-term measurement system consists of a total of 3 stations. The first station is located inside the church, where the sensors are located in the wall and in the pillar Figure 25.

Figure 25 Inside measurement station in St. Anna church

The other two sites are located north of the church. Here, two stations A and B are dug about 6 meters from each other. Station A is close to the church, station B is close to the church cemetery wall. The measurement data are then transmitted by cable from pit B to pit A, from where they continue through the church wall to the inner station. From there, the cable leads to the Campbell Scientific CR1000 data logger located inside the church in the stairwell.

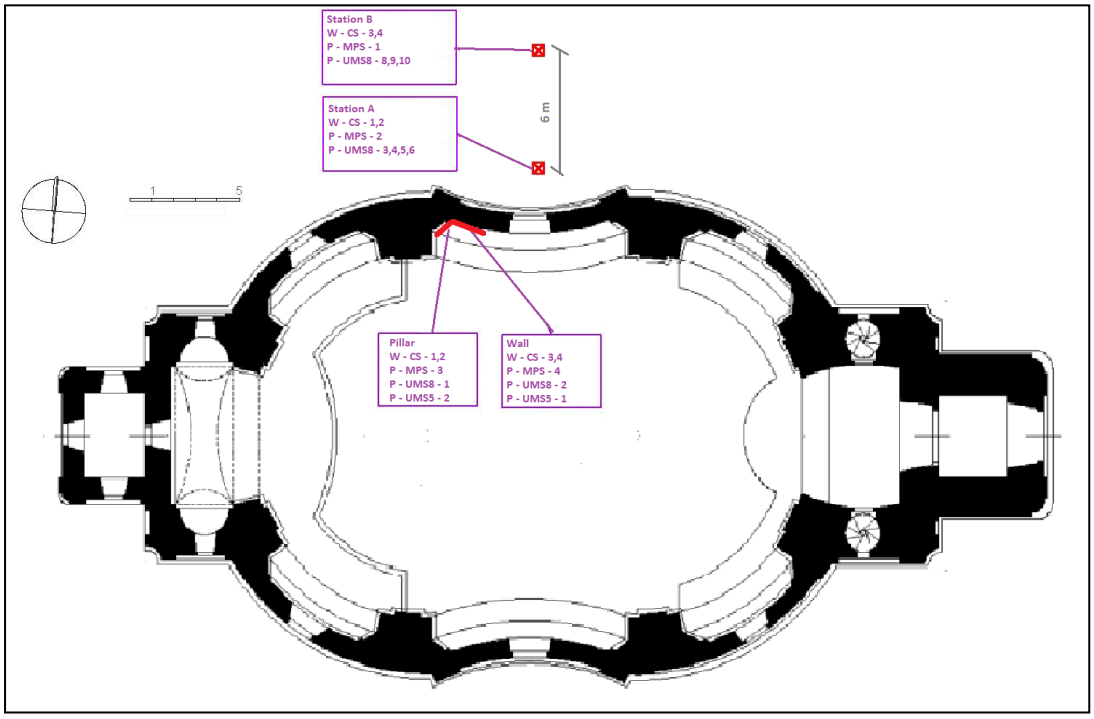

Figure 26 St. Anna church, Viznov, location of monitoring system

The location of the sensors at the various stations is shown in the above Figure 26. Here, in particular, the height arrangement can be seen in the following tablesTable 4,Table 5,Table 6,Table 7, andTable 8 . The height of the church floor has been chosen as a reference value and the remaining heights are related to it.

Table 4 T8 Tensiometer sensor location and depth/height Vižňov

T8	Location	Depth/Height (cm)
1	Pillar	22
2	Wall	37
3	Station A	31.6
4	Station A	57.9
5	Station A	76.5
6	Station A	109.9
7	Station B	surface
8	Station B	72.8
9	Station B	105.5
10	Station B	116.9

Table 5 CS 650 sensor location and depth/height Vižňov

CS 650	Location	Depth/Height (cm)
1	Station A	25
2	Station A	50
3	Station B	25
4	Station B	50

Table 6 CS 655 sensor location and depth/height Vižňov

CS 655	Location	Depth/Height (cm)
1	Pillar	20
2	Pillar	80
3	Wall	22
4	Wall	80

Table 7 T5 Tensiometer sensor location and depth/height Vižňov

T5	Location	Depth/Height (cm)
1	Wall	13.5
2	Pillar	13.5

Table 8 MPS-6 sensor location and depth/height Vižňov

MPS-6	Location	Depth/Height (cm)
1	Station B	10
2	Station A	10
3	Pillar	80
4	Wall	80

6.5 Characteristics of Measuring Instruments

The tensiometers UMS T8, UMS T5 (Meter Group, Germany) and MPS-6 sensors (Meter Group, USA) are used for measuring water potential. Volumetric water content is then measured with the CS 650 and CS 655 sensors (Campbell Scientific, USA). All sensors, with the exception of the UMS T5, additionally measure temperature.

Tensiometer UMS T8

UMS T8 measure the pressure component of the soil water potential in saturated and unsaturated media. A porous ceramic cup is used to transmit the water pressure from the soil to the water in the device, which allows them to come into contact with one another. The water in the device then transfers the positive and negative capillary pressures to the pressure sensor.

Over the winter the sensor can be kept in the ground, if the condition is met that the strain gauge cap is at least 20 cm under the surface. If the ground freezes, the strain gauge data will show a jump to a constant value, which is measured until the ground unfreezes once again, and then the measurement proceeds.

The pressure measurement range is between -85 kPa and 85 kPa with an accuracy of ± 0.5 kPa. Temperatures are then measured from -30°C to 70°C with an accuracy of 0.2 K for temperatures from -10°C to 30°C and 0.4 K for temperatures below -10°C and above 30°C, see Figure 27 .

The handy feature of the UMS T8 tensiometer is the refill pipes are situated on top of the device, where water can be added to the strain gauge without the need to interrupt the measurement and remove the strain gauge from the ground (Figure 27). [26]

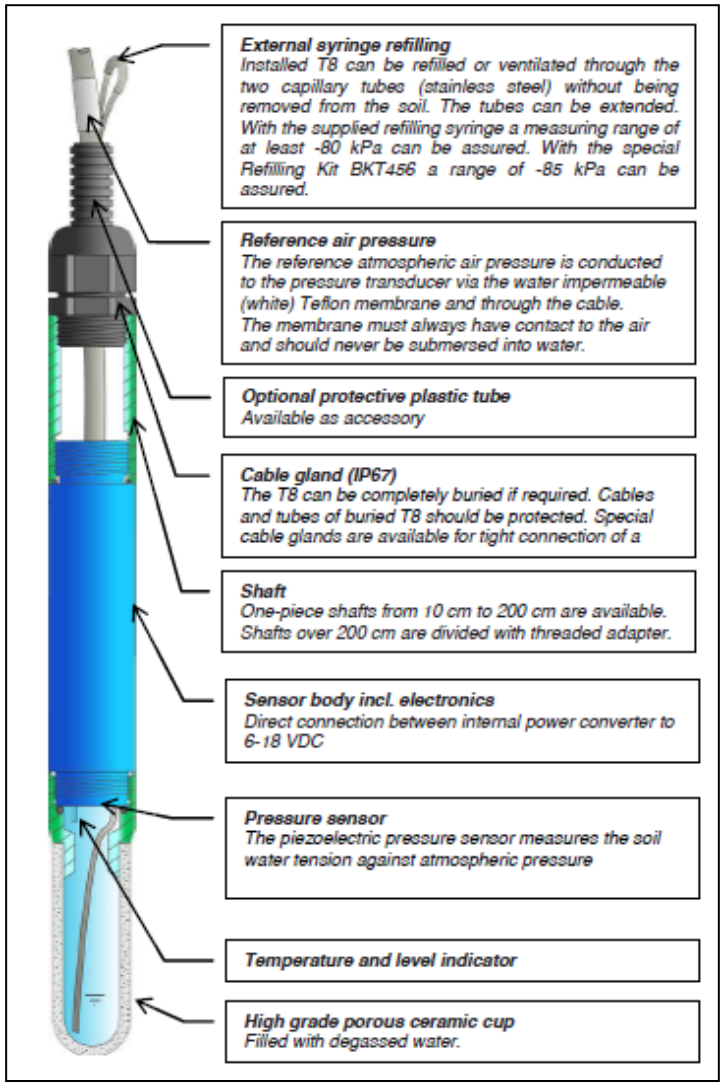

Figure 27 T8 Tensiometer composition [26]

Tensiometer UMS T5

The UMS T5 tensiometer is very similar to the UMS T8 tensiometer and thus works on the same basis. However, contrary to the UMS T8, it only measures pressures, not temperatures. In addition to the temperature sensor, the UMS T5 does not contain any water filling hoses. Nevertheless, its advantage lies in the small diameter of the measuring instrument body, which was used to measure

the water potential in the masonry of the St. Anna church in Vižňov (Figure 28). The length of the UMS T5 is 10 cm and the measurement range is from -85 kPa to 100 kPa with an accuracy of ± 0.5 kPa. [27]

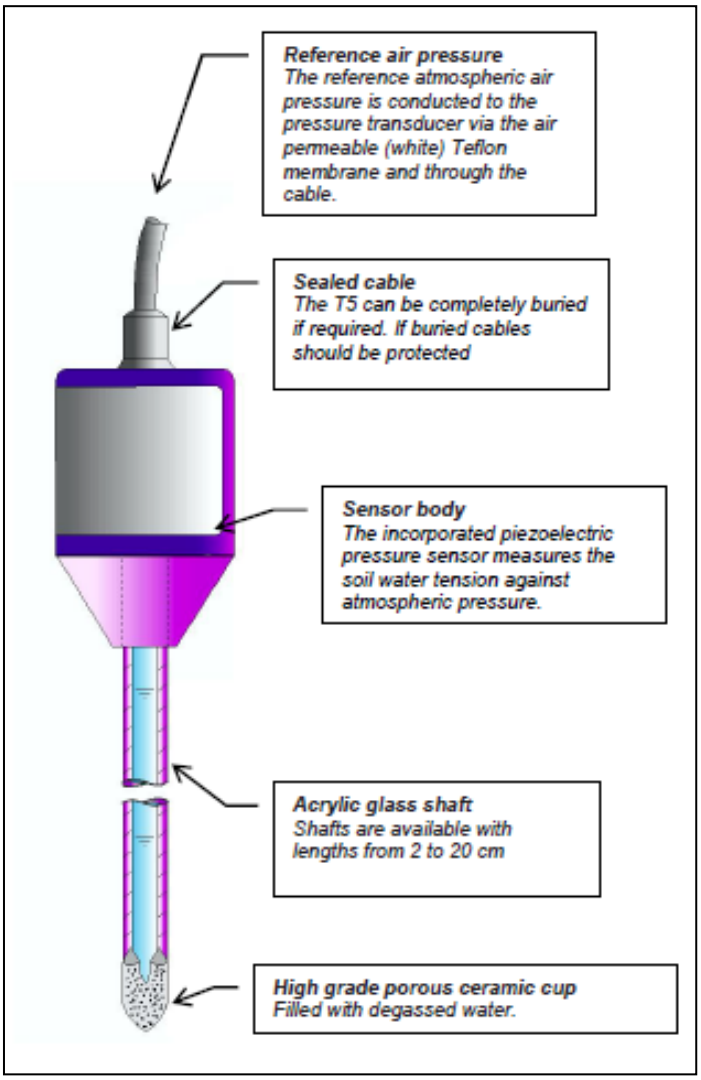

Figure 28 T5 Tensiometer composition [27]

CS 650/CS 655

The CS 650 moisture sensors by Campbell Scientific consist of two 30 cm long end caps of stainless steel connected to electronic circuits in an epoxy-coated housing. The CS 655 sensors also have two stainless steel needles connected to the printed circuit board but they are only 12 cm long. The instruments measure the electrical conductivity, water content and temperature values (Figure 29).

Determination of moisture is based on the principle of measuring the propagation speed of electromagnetic waves along the probe as a function of the changing permittivity of the soil

environment. An increase in the moisture content results in an increase in permittivity which reduces the propagation speed of the waves. The speed of propagation of the waves is obtained by measuring the time elapsed between the emission and return of the signal by a stainless steel needle. This velocity is then directly converted to humidity by volume using a calibration equation.

The temperature sensor is in contact with the tip of steel, but is inside the epoxy box. In the case of installation of the sensor in masonry, the temperature is measured at the surface rather than inside the masonry material due to the low thermal conductivity value of the steel and the small diameter of the tips.

For the CS 650 and CS 655 sensors, the water content measuring range is 5% to 50% with an accuracy of ± 3%. Temperatures are measured in the range -50°C to 70°C. With an accuracy of ± 0.1 °C for the temperature range 0°C to 40°C and an accuracy of ± 0.5 °C for temperatures above 40°C and below 0°C. [28]

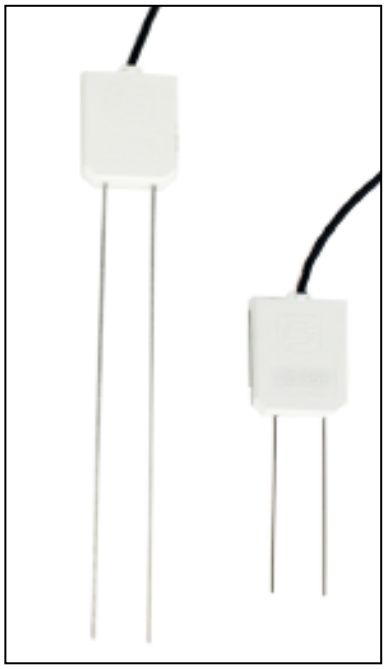

Figure 29 CS650 and CS655 sensors [28]

MPS-6

The MPS-6 pressure potential measuring instrument consists of two ceramic discs connected to a printed circuit board (Figure 30). The instrument also measures the temperature at the location of the ceramic disc. The pressure potential is measured on the same principle as that of the CS 650 and CS 655 sensors, i.e. by measuring the permittivity. In contrast to the sensors CS 650 and CS 655, the MPS-6 is measured on ceramic discs which are in equilibrium with the environment. The measuring range of the moisture potential is -9 kPa to -100,000 kPa with an accuracy of ± (10% of the read value + 2 kPa) in the range of values from -9 kPa to -100 kPa. The temperature measuring range is then from -40 °C to 60 °C with an accuracy of ± 1 °C. [29]

Figure 30 MPS-6 Sensor [29]

6.6 Precipitation Measurement

In October 2016, a continuous rain gauge was installed in the cemetery area adjacent to the church of All Saints in Heřmánkovice to continuously measure rainfall at the site. The advantage of the rain gauge is that is heated which allows long-term measurements, including during the winter period. The rain gauge was placed in an open area at a sufficient distance from the nearest trees and other potential obstacles, approximately 50 m northwest of the church building. The data measured by the rain gauge was also collected by a Campbell Scientific CR 1000 data logger inside the church and recorded in a 30-minute time step.

On the property adjacent to St. Anna's Church is a rain gauge belonging to the Regional Hydrological Information System, which provides free online data and the measurement starts from July 14, 2017. The data from the rain gauge at Vižňov had to be adjusted first, as the total precipitation is measured here in a six-minute step.

This page is left blank on purpose.

7. MEASUREMENT RESULTS AND DISCUSSION

This chapter presents the results of the monitoring system already presented and described in chapter 6.4 along with comments and discussion to each specific data. The results of the monitoring system are data related to temperature, water content and water potential recorded for a long term duration, between September 2016 and May 2020 for All Saints church in Heřmánkovice, and between July 2017 and May 2020 for St. Anna church in Vižňov. All the results are presented in the Annexes at the end of the report due to the big size of the plots.

7.1 All Saints Church, Heřmánkovice

7.1.1Temperature

Temperature readings must be taken into account before evaluating the measured values of water content and potential. All the sensors used measure the temperature simultaneously, but each at a different location. The temperature sensor inside the CS 650 sensor is located near the exit of the needle at the surface, so it does not measure the temperature inside the material but at the surface (Annex 1 & 2). For the Decagon MPS-6 potential sensors, the temperature is also measured at the surface of the sensor, but since the sensor is located entirely inside the material, the temperature value is more relevant (Annex 5). The best situation is for T8 tensiometers, where the temperature sensor is located directly inside the ceramic cup (Annex 7).

The temperature data from the CS650 sensors were divided into two plots (Annex 1 & 2), one for the temperature inside the church and the other for the data measured at soil stations A and B outside the structure. With regard to the data from the outdoor measurement, it is evident that the temperature at different depths and at different locations in station B is always higher than the temperature in station A. This is well seen, for example, in the CS650 sensors at a depth of 49 cm in station B and 50 cm in station A, which have an almost identical path at a constant difference of about 0.7 ° C for example during the spring of 2018. The obvious reason for this observation is the fact that Station A is closer to the church, where it is shaded for most of the day, than Station B, which is further away. Therefore, it is expected that there will be less opportunity for evaporation near the building and therefore more moisture accumulation. Some other observable characteristics are as well as expected: in the soil, we find that the values measured by the sensors fluctuate much closer to the earth's surface, with the fluctuations decreasing in depth (Annex 1).

Inside the church and in masonry, we see the most fluctuating values of the CS650 sensors, which measure on the surface of the masonry, less fluctuation of the MPS-6 potential sensors in the masonry surface layer and a T8 strain gauge inserted obliquely into the foundation at a depth of 28 cm below the ground gives the by far smoothest path.

For the winter period, where freezing can occur and can cause problems with all sensor readings. For the ground sensors, the temperature did not fall below 0°C during the entire duration of the sensor readings (some exceptions for the CS650 during winter 2018). But for the potential sensors (MPS-6), the temperature did fall below 0°C during all winter seasons at shallow depths. The values measured by these sensors should therefore be valid. In addition, one can see the relationship between precipitation and temperature, where during the winter the precipitation is negligible because of snow and therefore the temperature is about 0°C. Another link with precipitation, when after a major precipitation event the temperature drops rapidly.

7.1.2Water Content

Water content is only measured using the CS650 sensors, and the same as the temperature results, the water content plots are split in two. The first for the water content inside the church and the second for the outside environment at the ground stations. The presentation of the water content results focuses on any major changes in value and, to be more precise, these events occur with the change in temperature and precipitation, so the objective is to verify the results in each season, mainly in winter, spring and fall.

First of all, starting with the fall season, during the month of October specifically between October 22 2016 and October 14 2016, also September 23 2017 - October 06 2017, October 26 2018 - October 30 2018 and, October 08 2019 - November 18 2019, we notice that during these periods we have an significant jump of water content with the beginning of the high amounts of precipitations (11mm/day - 18 mm/day). At station A, we observe a very fast reaction and a sudden jump in water content to values in which the measured water content then shifts for most of the subsequent measurement. At station B, saturation occurs much more slowly. We first observe a gradual increase in water content in the area of the shallowest sensor, and once the rainfall intensity increases, the deepest sensor is affected and a similar jump occurs. From this point on, the water content increases even in the deeper layer. After this initial wetting each year, the values of each sensor evolve around the same values. Station B's area reacts in particular, and logically especially its upper layer, in such a way that it always gets wet quickly and the water drains off easily. In station A, the water tends to accumulate and the soil remains almost saturated.

Between December and January (winter), reactions to precipitation stop when the air temperature drops below zero and the precipitation turns into snow. Without subsidies for liquid precipitation, the soil moisture in all sensors decreases very slowly. In addition, due to freezing, the CS650 sensors do not function properly, so filtering was necessary, but for the winters 2019 and 2020 the temperatures did not lead to freezing for both soil and walls.

After the temperature has risen to positive values at the end of February and beginning of April (spring), the water content values gradually returned to the previously observed values and during the rest of the period they react to precipitation in the same way as in the fall season (Annex 3).

In the case of sensors located in the masonry, we do not observe any valid movement of the measured values in the fall. In winter, we observe a significant drop in the values, which manifests itself especially in the winter of 2020. Sensor stoppage also occurs when temperatures fall below zero, and we can observe a lack of data due to data filtering during the following periods: winter 2017, 2018 and 2019. When the temperature returns to positive values in the beginning of March (spring), the measured water content values also return.

After the pause during winter, the sensors in the pillar and in the wall at a height of 10 cm above the ground remain at approximately the same value again. In the sensors located at a height of 60 cm in the pillar and in the wall, we see a steady, gradual increase in the values. So it seems that with the spring melt, a little more moisture will seep into the upper layers of the masonry. In Annex 4 we see that the moisture values are already stable; a slightly lower moisture content was measured in the niche than in the column. In both places, as expected, we observe higher moisture content in the sensor located under the floor.

7.1.3Pressure Head, Tensiometer

At the beginning of the measurement period, a gradual increase of pressure heads of the soil is observed. Especially at station B, we observe reactions at individual depths ranging for a couple of months (September - December) in the case of the deepest sensor. This phenomena is occurring each year approximately at the same time. It should be noted, however, that the values measured at the site which are irregular are close to the limit of the measurement range declared by the manufacturer, which is around 85 kPa.

The jump in values at the T8 sensors and the return to the previous trend are certainly related to the refilling of the sensors, and this happens when the soil gets drier than -85 kPa, and the tensiometer leaks. In station A, in response to a major precipitation event, a very rapid increase in values at all depths was observed. A much faster response in this habitat is probably favoured by a greater saturation (significantly higher measured humidity) before precipitation. However, due to the degree of difference with the second habitat, even more influences can be expected. This may be due to water flowing into this area from higher elevations (in Station B, however, surface runoff has not been confirmed), or because the church here may well function as a "stop" in the runoff.

As anticipated, the shallow sensors with the highest degree of reaction react the fastest, while the deepest ones reactions are only slower. This applies to Station B for all precipitation events. At Station A, however, the behaviour described is only observed in precipitation of lower volume. In contrast, a sensor located at a depth of 109 cm in station A shows by far the most significant response to the most important precipitation events (specially 2018). This would correspond to the fast connection of the surface with the sensor measuring point at this location, which is also reflected in other phenomena already described. We observe the described reactions up to the precipitation of snowfall and again even after warming in spring (Annex 8).

7.1.4Water Potential Sensors

In the soil, measurements are taken at station A on the sensor at a depth of 11 cm and at a depth of 10 cm between stations A and B (station C). The measured initial value for sensor A corresponds relatively well with the values measured by the strain gauges. The sensor between the stations cannot be compared well with any of the strain gauges (tensiometers). The sensor at station A with the depth of 11 cm has the same profile as the tensiometer sensor at the depth of 41 cm, it is easy to notice the same reactions of both sensors at the same time but with different magnitudes due to the difference of depth.

The only other information coming from the values measured by these sensors in the ground is their behaviour when the temperature drops to freezing point. Since the manufacturer declares a malfunction of the sensors at temperatures below 0°C due to the different permittivity of water and ice, a filtering was made regarding measured values going out of the measuring range. At the same time, it is verified that the sensors function normally again after the environment has thawed. The temperature in the ground oscillated just around the freezing point throughout the winter seasons, and the measured potential reading, based on this oscillation, tended to fall outside the actual values and return to them.

The fluctuations seen in summer 2018 and 2019 are related to the dry weather happening with the small amount of precipitation, thus the zone where the sensors are located is extremely unsaturated and the flow of water is very low. Also, it can be noticed for the sensors inside the church where a small fluctuation is happening for the same reason. Thus the sensors are working normally during these periods (July - September 2018 and July - August 2019) with a maximum value at pit C equal to 2350 kPa and 1489 kPa at pit A at 10 cm and weren't functioning correctly in the summer of 2017 where the same atmospheric conditions existed (Annex 6).

Note: The values of the pressures for both MPS-6 and T8 sensors were multiplied by (-1) in order to see better the results in the plots. Thus the positive values in the figure were originally negative.

7.2 St. Anna Church, Vižňov

7.2.1Temperature

With the exception of T5 tensiometers, temperatures are measured by all sensors. CS650 sensors are used to measure the temperature in the soil stations A and B, CS655 sensors are located inside the church. Furthermore, MPS-6 and T8 sensors also record temperature values (Annex 13 & 15), and as discussed in chapter 7.1.1 the accuracy of each sensor is well known and its reliability.

Starting with temperatures from the outdoor environment, from the CS650 sensors at station A (Annex 9) it is possible to observe a practically identical course of temperatures at depths of 25 and 50 cm with a difference of approximately 1 °C, and the temperatures at station B for the same depth is always higher, thus more moisture is present at station A due to the slope of the ground and because station A is closer to the church. In addition, another identical course of temperatures can be noticed from T8 sensors at depths of 31.6 and 57.9 cm at station A, where the difference between the layers is approximately 0.7 °C. The course of temperatures at a depth of 109.9 cm and 31.6 cm is similar. Depending both on the temperatures and on the pressure potential values interpreted in the following point, it can be estimated that a layer of low permeability exists at a depth of between 65 and 80 cm. This may explain a similar temperature profile at depths of 32 and 110 cm. The sensor located at a depth of 110 cm is influenced by the groundwater flowing at this location from the upper layers of the slope above the church.

According to a survey done by CTU researchers, it was found that a ditch is located at station A, approximately 30-40 cm deep, in which water swells during precipitation, which then remains in the ditch for a very long time. Temperature fluctuations at a depth of 58 cm, identical to a depth of 32 cm, are caused by the presence of this ditch.

From the CS655 sensors (Annex 11), it is noticed that the temperature profiles are approximately the same in values, the difference between the location at 20 cm and 80 cm is negligible and the fluctuations are really high because the CS655 sensors measure the temperatures at the surface.

7.2.2Water Content

The graph from (Annex 10) shows that in station A, the soil is wetter than in station B, in both depths. It can be seen that the sensors at station B react to precipitation more than at station A and the sensor at depth of 50 cm at station A doesn't react much for the whole monitoring period it only varies between 0.498 to 0.547 m^3/m^3, which is weird and ask for a questioning if the sensor is working correctly and it can be explained due to the high saturation of the soil during the entire period, thus no

significant increase or decrease is observed in the moisture. For the rest of the sensors it is possible to see the drop in water content when the drier periods are present (summer).

The same situation with freezing is present in Vižňov, the data is removed during winter due to the stoppage of the CS650 and CS655 sensors. Fluctuations are appearing at both stations at the depth of 50 cm, due to the saturation of the soil and it is obvious by comparing the data between both churches, since the water content in Vižňov varies between 0.4 and 0.6 m^3/m^3 while in Heřmánkovice it barely reaches 0.4 m^3/m^3.

The values measured inside the church (Annex 12) show that the most significant contact between the interior and the exterior takes place at the base of the wall. The relatively high value of the masonry moisture in the pillar and wall at the depth of 80 cm, when the humidity is around 11% 17% in the whole period, proves that there is a significant rise of water from the space under the foundations. One of the causes of higher masonry water content is the fall of sandstone blocks from the outside of the building, which results in the revealing of the masonry surface, weathering of mortar and masonry, and above all facilitates contact between masonry and soil.

7.2.3Pressure Head, Tensiometer

In this chapter, the measured data will be interpreted obtained by the tensiometers T8 (Annex 16). Regarding the T5 tensiometer there was a failure in the measurement which is interpreted by values that are out of range and by the absence of reactions of the sensor to specific events such as variation of temperatures, precipitation events, variation of water content. Thus, the data of the T5 sensors showed that there is a malfunction that cannot be explained how it exactly happened.

For the dry periods (summer), it can be seen that there is a significant fluctuation in moisture in the pillar, which is evident from the decrease in pressure in the summers varying from -5 to -80 kPa and the subsequent sharp increase after the start of precipitation. At the base of the wall, such significant fluctuations in pressure heights do not occur, but the values indicate the practically permanent presence of pressurized water in this area.

From the measurements of the T5 sensors (Annex 17) placed in the structure at a height of 20 cm above the ground, it is again possible to observe greater fluctuations in the water content in the pillar than in the wall. However, the wall is considerably more humid than the pillar. But, still the results from the T5 sensors are not reliable.

After the summer periods, there are no longer such fluctuations in pressure heights as in the summer. The groundwater level below the foundations remains at approximately the same level. can be read

that there is, as in the summer, pressurized water under the wall. Under the pillar, the groundwater level is again held at a small depth below the floor, but does not reach the surface. The wall is also wetter than the pillar in winter than it was in summer.

Regarding the sensors outside the church, during the dry period,at station A a very similar course of pressure heights can be observed at depths of 57.9 cm and 109.9 cm, thus a same permeablity layer is available at both depths. The sensor at a depth of 57.9 cm is affected by both the accumulation of the water in the ditch and the inflow and by outflow of water from the area along the inclined layer of insulation. Depth pressure height values 109.9 cm are then affected by the inflow of water into the area of the insulator below this horizon and again also by the inflow of water from the soil layer at a depth of 76.5 cm.

The infiltration of precipitation in station B is little affected by the occurrence of several layers permeable soils. Measured values potential confirm this statement and further clarify it. In the fall periods, the same course of pressure heights can be seen again in station A at depths of 57.9 and 109.9 cm in the graph of total potential, as in the summer. In station B, it is possible to observe a similar course of pressure heights at depths 105.6 and 116.9 cm, when the sensors practically do not react to precipitation.

7.2.4Water Potential Sensors

The values from the MPS-6 sensors (Annex 14) do not correlate with the values obtained with the T8 tensiometers. For the sensor in station A at 10 cm depth, the values recorded for the whole monitoring period untill May 2020 are somehow constant around 9 kPa, thus the sensor is not functioning and it is totally different than the T8 sensor at the depth of 31.6 cm. Concerning the sensor in station B at 10 cm also has a different path comparing it with the T8 tensiometer at the surface. For the sensor at 10 cm fluctuations are available between May and October 2018 and in July 2019 but for the Tensiometer the value is near Zero which makes it saturated during the whole time.

For the sensors located inside the church, the same problem is also there, for both pillar and wall the measured datas do not comply with the T8 sensors. The data measured by sensors inside the church have a non-standard course, which is caused by an error that has not yet been identified.

Note: The values of the pressures for both MPS-6, T8 and T5 sensors were multiplied by (-1) in order to see better the results in the plots. Thus the positive values in the figure were originally negative.

This page is left blank on purpose.

8. MODELLING OF WATER TRANSPORT

The objective of the modelling of the water transport is to present the current state of the walls of both churches. The aim was to replicate and extend the modelling efforts presented by [23]. Thus, a steady state simulation was carried out using Hydrus 3.0x software. Hydrus is a software for simulating the movement of water, heat, and solutes in two and three dimensional porous media with variable saturation [30]. The Hydrus program numerically solves the Richards Equation for variable saturation water flow and advection-dispersion equations for both heat and solute transport. For this modeling only water flow modelling is taken into account. The modelling done in this study is similar to the one done in [23], where it is the same modelling of the wall of the church in Heřmánkovice but with a diferent modelling tool that will lead in this study to model also the wall of St. Anna in Vižňov.

8.1 Material Characteristics

The 2D modelling of the walls is defined with the hydraulic characteristics of the sandstones only, without taking into consideration other probable filling materials and mortar. Thus the study depends only on the characteristics of the sandstone samples from each church.

For the All Saints church, three samples of sandstones were taken to the lab. The saturated water content of the sandstone samples was measured gravimetrically based on the saturated weight after 7 days of free capillary rise from an open bath and the dry weight after oven drying at 105 °C at a constant weight. The main drainage branches of the retention curves (Figure 14) were determined using standard methods for sandboxing and extractor pressure. The masonry 's saturated hydraulic conductivity was determined in-situ using a tension minidisk infiltrometer from the church wall on a large block of sandstones [23]. One of the samples characteristics was chosen for the wall modelling.

Regarding the St. Anna church in Vižňov, the same procedure was carried out but for 5 samples and at the end a scalled value for the hydraulic characteristics was obtained [31]. Obtaining the parameters was needed to express the retention curves by van Genuchten's formula, which is also the same formula used by Hydrus software to implement the properties for the calculation (Table 9).

Table 9 Hydraulic characteristics of sandstone for both churches [31] [23]

Church	θ_r ($cm^3\,cm^{-3}$)	θ_s ($cm^3\,cm^{-3}$)	α (cm^{-1})	n (–)
All Saints	0.00	0.27	0.009	1.13
St. Anna	0.10	0.29	0.057	1.134

8.2 Geometrical Representation of Masonry Wall

The vertical cross-section of the two walls was represented by a rectangle 1 m wide and 13.2 m high rising 12 m above the ground and 1.2 m below the ground (Figure 31). Which is the exact situation in All Saints church foundations depth and was taken as an assumption for St. Anna since no investigation regarding its foundations was done. The design area was discretized using a triangular finite element mesh with a size of 2 cm for each element consisting of a total of 51,793 nodes and 102,164 elements (Figure 32).

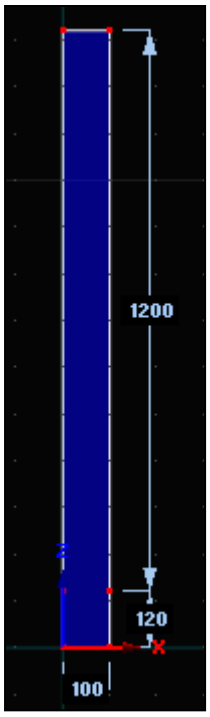

Figure 31 Model dimensions

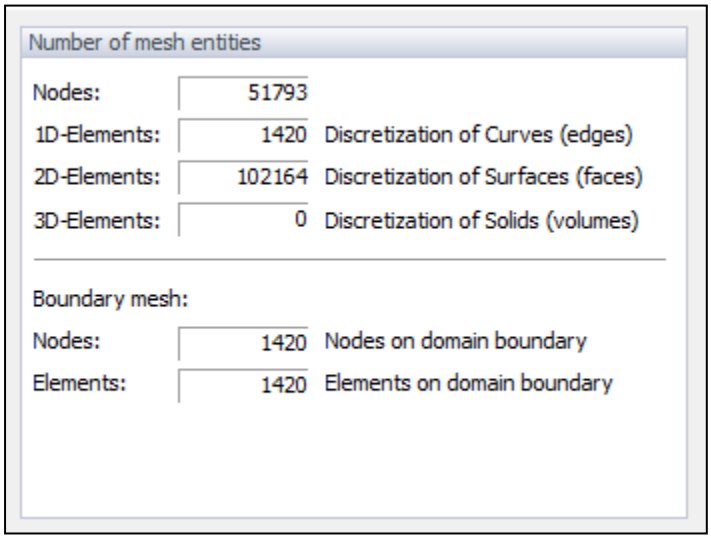

Figure 32 Model mesh information

8.3 Steady State Simulations

Steady state simulation are made to show the current state of the churches walls. For the All Saints church saturation is assumed at the bottom of the wall at the foundations level, while for St. Anna the saturation is assumed at the ground surface since it is noticed from the monitoring system that the wall is saturated at the soil surface for the whole period of monitoring.

In order to obtain steady state of the walls, a pressure head is applied on both sides of the wall above the ground surface of a value of -15,000 cm. Where this value represents the second stage of evaporation, In the second evaporation stage, the actual evaporation is considerably reduced below

the potential rate, being controlled by the unsaturated hydraulic conductivity of the drying wall surface. During this stage, the potential of the surface water drops to extremely low values, close to equilibrium with the humidity in the air. In addition, for the sides of the wall beneath the surface, a constant pressure head equal to 0 cm is applied for the whole 1.2 m and at the bottom of the wall, also, no flux is applied at the top of the wall.

8.4 Results

For the All Saints church, the steady state is achieved after an analysis of 8000 days long, where no difference in the results occur after this time duration. The water content values stay the same at this moment and thus represents the current state of the walls.

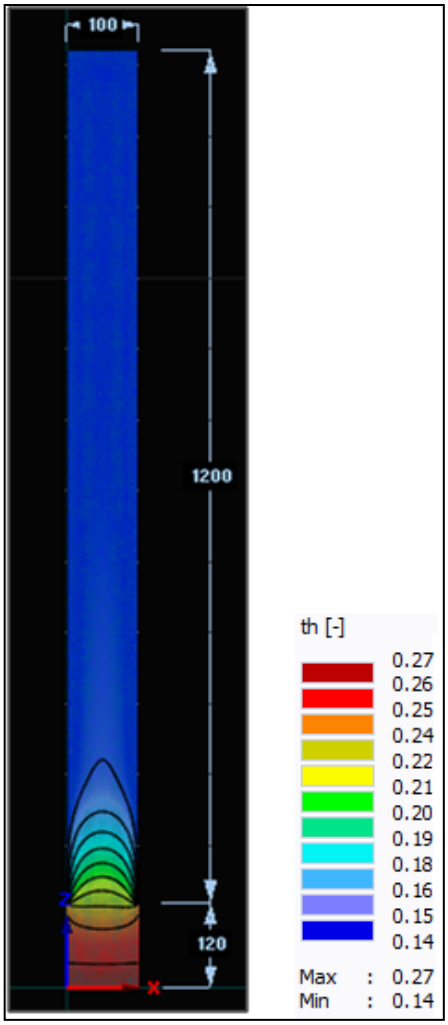

Figure 33 Water content values for the wall of All Saints church

The values of water content obtained from the Hydrus simulation (Figure 33) correlate with the analysis made by [23] regarding the same type of analysis for the steady state.

The modeled wall of St. Anna's church reaches its current state in Hydrus after 15,000 days of simulation, and the wall is much more wet than in All Saints and it makes sense since the ground surface is saturated (Figure 34). The difference in water content can be easily seen between the two walls, at the top of the St. Anna's wall the water content is approx. 0.17 cm^3 cm^{-3} while for All Saints it is 0.14 and also around the ground surface the higher values can also be seen for the church in Vižňov.

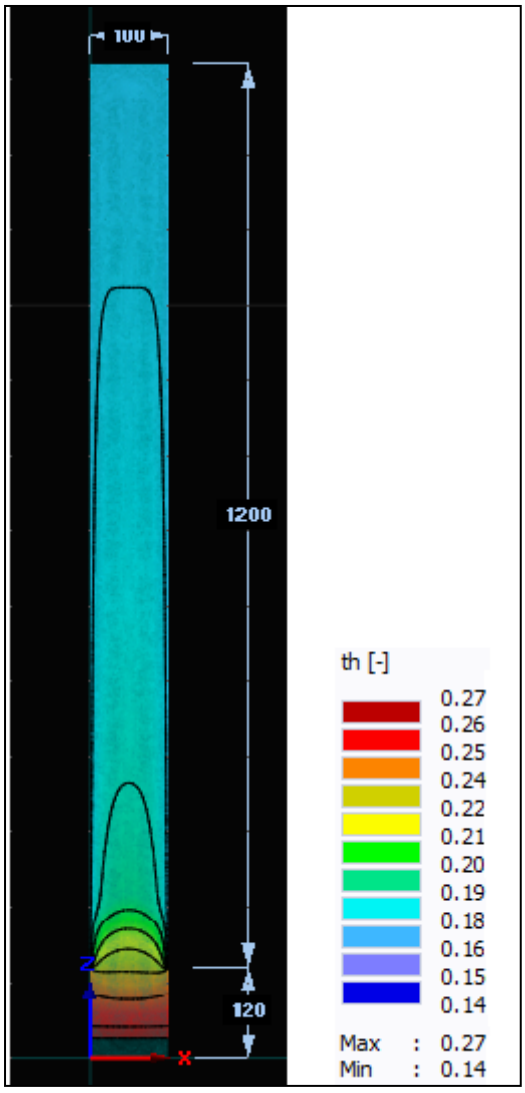

Figure 34 Water content values for the wall of St. Anna church

9. RECOMMENDATIONS

Based on the data from the monitoring system related to water content and pressure potentials, and on the modeling of the water transport of walls in Hydrus it is clear that several measures will be needed to improve the current situation.

First of all, a drainage system will have to be built along the north side of the churches which should lead to a reduction of the water table around the foundations of the masonry. After partial drying of the masonry, ideally after the summer, it will be necessary to install blocks of stone, which will be grouted with waterproof mortar, which should limit the flow of rainwater from the ground surface horizon into the church masonry.

For the All Saints church, Water evacuation from the adjacent area north of the church could be done by installing a drain that copies the entire north side of the church, with a reasonable slope of about 1 percent from the highest point above the north wall centre. Because of the shape of the church and the need to copy this shape, it would be appropriate to make the drain from a flexible PVC or PE pipe according to [32] at least 100 mm in diameter with a gravel backfill as specified by the manufacturer.

As far as St. Anna Church is concerned, the same type of drainage system can also be used, but as the amount of moisture is higher, another type of solution is more appropriate. The possibility of building a ventilation system for masonry foundations, which is described in Chapter 5.3, should be considered [13]. The reduction of the groundwater level, combined with the increase in masonry evaporation due to the evacuation of moist air from the foundations, could lead to a significant improvement in the current state of the masonry.

Finally, these solutions solve the problems facing the churches and represent interventions that doesn't affect the integrity of the structures, and follow the concept of minimal interventions related to historical constructions. Thus, the study points out the problems governing the historical structures in the Broumov region and their actual state of conservation with a possibilities of solutions.

This page is left blank on purpose.

10. CONCLUSION

The work analyzed the water temporal and spatial distribution in the walls of the 18th century baroque churches of All Saints (in Heřmánkovice) and Saint Anna (in Vižňov) and in the soil surrounding them. The monitoring system consisted of water content sensors, tensiometers and water potential sensors.The monitoring started in 2016 for All Saints church and in 2017 for Saint Anna's church.

From the monitoring system it was possible to get a clear idea about the amount and effect of water transport inside and around the churches. Both structures are clearly affected by the high amount of water content which is degrading the masonry and is a source of possible biological colonization. Regarding St. Anna it was found that the soil is saturated due to the high values of water content during the whole period (approx. 0.5 m^3m^{-3}). On the contrary, for All Saints the water content obtained at the bottom of the wall from the CS650 sensors was variating with time and would fall in the range of 0.15 - 0.2 m^3m^{-3} which is less than half of the amount in St. Anna's church.

In addition, a modelling of the water transport was carried out to obtain the current state of the walls of both churches which gave us a better understanding of how the current moisture distribution in the walls developed. For the All Saints church, steady state occured after 8,000 days of running the analysis, and for St. Anna, steady state was reached after 15,000 days. The time is higher to reach steady state in St. Anna due to the higher presence of moisture. And from the modelling the value of water content at the top of the wall in Vižňov is 0.17 m^3m^{-3} while for Heřmánkovice it is 0.1 m^3 m^{-3}.

It is recommended to ensure a reduction in the ground water level in order to protect and preserve the historical constructions. One of the simplest methods of reducing water content is an open drainage system, that doesn't require much maintenance and cost. Second, a ventilation system can also be used, in the case of St. Anna because of the higher levels of moisture.

Finally, a better understanding of the situations of the churches are now acquired. The water migration paths from the soil to the masonry are well known after the analysis of the data from the monitoring system and the water transport simulations.

References

[1] “Historical building surveys.” https://www.npu.cz/en/NPU-and-heritage-conservation/NPU-the-institution/services/historical-building-surveys (accessed Apr. 19, 2020).

[2] “Ottokar II of Bohemia - Wikiwand.” https://www.wikiwand.com/en/Ottokar_II_of_Bohemia (accessed Apr. 19, 2020).

[3] “Gascoigne, Bamber. ‘History of Bohemia’ HistoryWorld. From 2001, ongoing.” http://www.historyworld.net/wrldhis/PlainTextHistories.asp?groupid=2617&HistoryID=ac40&gtrac (accessed Apr. 30, 2020).

[4] D. Gerson, “Baroque Architecture Explained – 16th - 18th Century — Gentleman’s Gazette.” https://www.gentlemansgazette.com/baroque-architecture-guide-explained/ (accessed May 02, 2020).

[5] J. Kotalík, *Architektura barokní*. Praha: Správa Parž ského hradu, 2001.

[6] M. Broumov, “The Region Of Broumov,” 2003. http://arch.broumov-mesto.cz/verze/b_gb_region.html (accessed May 02, 2020).

[7] “The Broumov Group of Churches.” Accessed: May 03, 2020. [Online]. Available: https://www.broumov.net/assets/File.ashx?id_org=1277&id_dokumenty=1010.

[8] R. F. Craig, *Soil Mechanics*, Sixth Edition. Taylor & Francis e-Library, 2004.

[9] W. A. Jury and R. Horton, *Soil Physics*. 2004.

[10] R. Lal and M. K. Shukla, *Principles of Soil Physics*. 2004.

[11] M. P. Anderson and W. W. Woessner, *Applied Groundwater Modeling Simulation of Flow and Advective Transport*, vol. 4. 2002.

[12] Y. Mualem, “A new model for predicting the hydraulic conductivity of unsaturated porous media.,” 1976.

[13] E. Franzoni, “Rising damp removal from historical masonries: A still open challenge.,” *Constr. Build. Mater. 54123-136*, 2014.

[14] P. B. Lourenço, E. Luso, and M. G. Almeida, “Defects and moisture problems in buildings from historical city centers: a case study in Portugal.”

[15] F. Tariku, K. Kumaran, and P. Fazio, “Integrated analysis of whole building heat, air and moisture transfer,” *Int. J. Heat Mass Transf. 53 3111–3120*, 2010.

[16] M. Qin, G. Walton, R. Belarbi, and F. Allard, “Simulation of whole building coupled hygrothermal-airflow transfer in different climates,” *Energy Convers. Manag. 52 1470–1478*, 2011.

[17] G. H. dos Santos and N. Mendes, “Simultaneous heat and moisture transfer in soils combined with building simulation,” *Energy Build. 38 303–314*, 2006.

[18] J. Berger, S. Guernouti, M. Woloszyn, and C. Buhe, “Factors governing the development of moisture disorders for integration into building performance simulation,” *J. Build. Eng. 3 1–15*, 2015.

[19] M. I. M. Torres and V. P. de Freitas, “Treatment of rising damp in historical buildings: wall base ventilation,” *Build. Environ. 42 424–435*, 2007.

[20] F. Sandrolini and E. Franzoni, “An operative protocol for reliable measurements of moisture in porous materials of ancient buildings,” *Build. Environ. 41 1372–1380*, 2006.

[21] D. D’Agostino, “Moisture dynamics in an historical masonry structure: The Cathedral of Lecce (South Italy),” *Build. Environ. 63 122-133*, 2013.

[22] Z. Pavlık, P. Michalek, M. Pavlıkova, I. Kopecka, I. Maxova, and R. Cerny, “Water and salt transport and storage properties of Msene sandstone,” *Constr. Build. Mater. 22 1736–1748*, 2008.

[23] T. Vogel, J. Dusek, M. Dohnal, and M. Snehota, “Moisture regime of historical sandstone masonry — A numerical study,” *J. Cult. Herit. 42 99–107*, 2019.

[24] “AOPK CR.” https://www.ochranaprirody.cz/ (accessed Jun. 12, 2020).

[25] “Map applications - Czech Geological Survey.” http://www.geology.cz/extranet-eng/maps/online/map-applications (accessed Jun. 12, 2020).

[26] “T8 Manual Long-term monitoring Tensiometer.” 2012.

[27] “T5 Manual Pressure Transducer Tensiometer.” 2018.

[28] “CS650 and CS655 Water Content Reflectometers.” 2018.

[29] “MPS-2 & MPS-6 Dielectric Water Potential Sensors Operator’s Manual.” 2016.

[30] M. Šejna, J. Šimůnek, and M. Th. van Genuchten, “The HYDRUS Software Package for Simulating the Two- and Three-Dimensional Movement of Water, Heat, and Multiple Solutes in Variably-Saturated Porous Media.” 2014.

[31] Oldřich Peleška, “ASSESSMENT OF THE WATER TRANSPORT IN A SOIL-MASONRY SYSTÉM OF THE BAROQUE CHURCH OF ST. ANNA IN VIŽŇOV,” Czech Technical University in Prague, Czech Republic.

[32] “Flexible drainage pipes with geotextile.” http://www.stavebni-cenik.cz/47-informace/informace/130-flexibilni-drenazni-trubky-s-geotextilii (accessed Jul. 08, 2020).

[33] “Mapy.cz.” https://en.mapy.cz/zakladni?x=-8.3523000&y=41.2493000&z=10 (accessed Jun. 12, 2020).

[34] “VÚMOP Research Institute of Land Reclamation and Soil Protection, vvi.” https://www.vumop.cz/ (accessed Jun. 12, 2020).

ANNEX

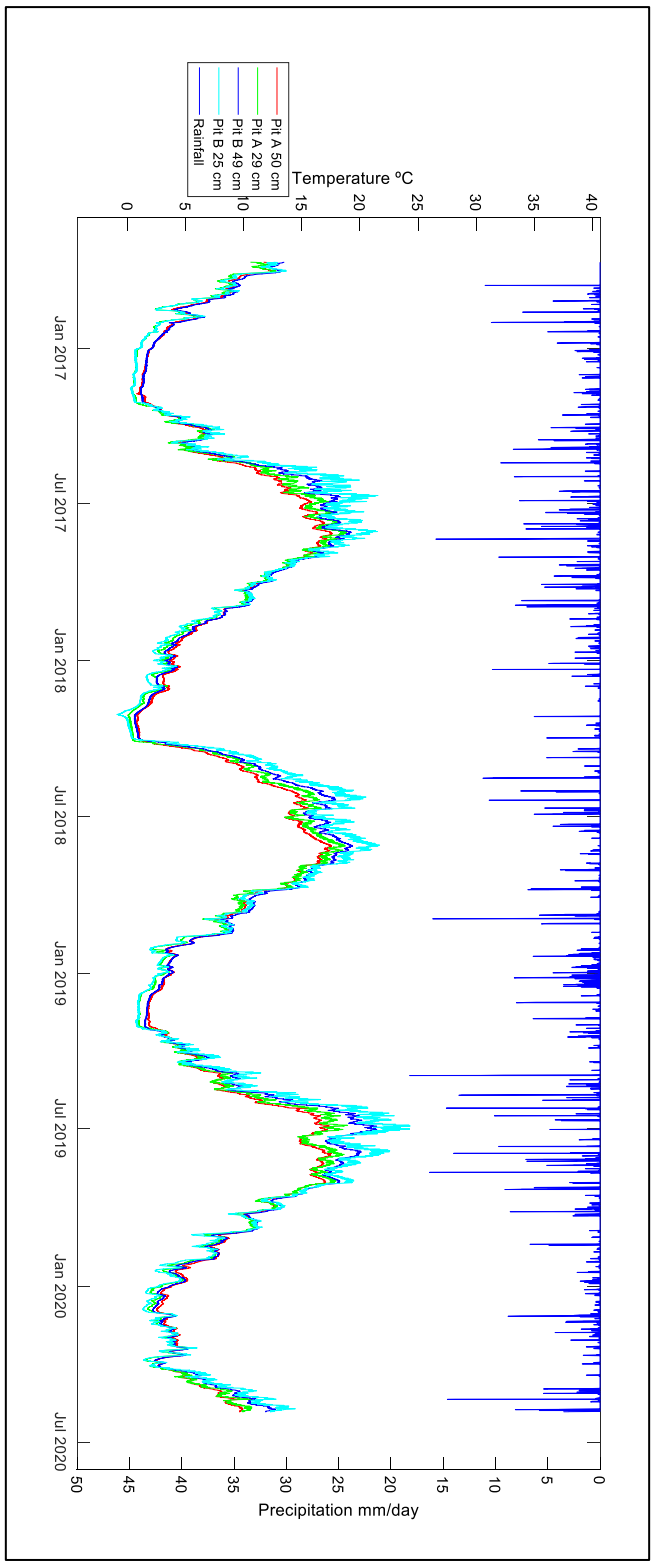

Annex 1 Temperature of CS650 in the soil and rainfall plot, Hermankovice

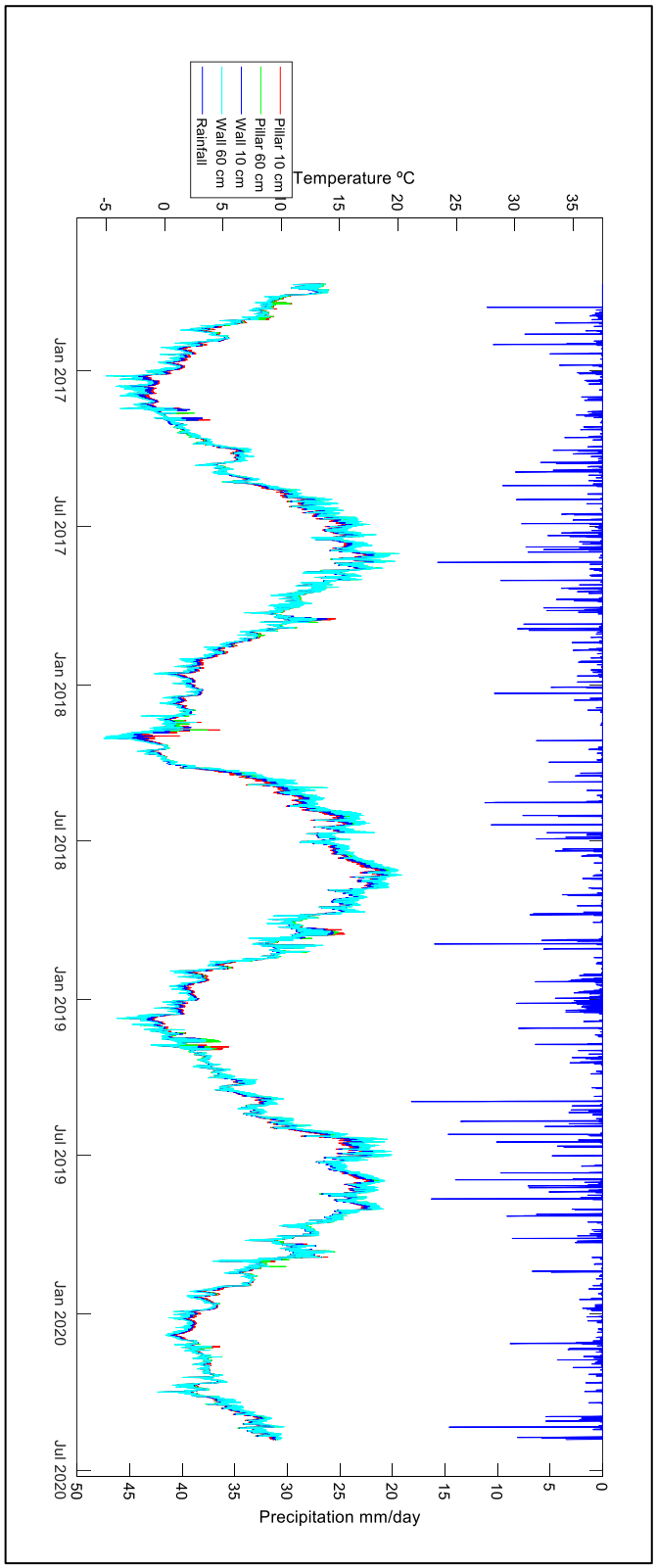

Annex 2 Temperature of CS650 in the church and rainfall plot, Hermankovice

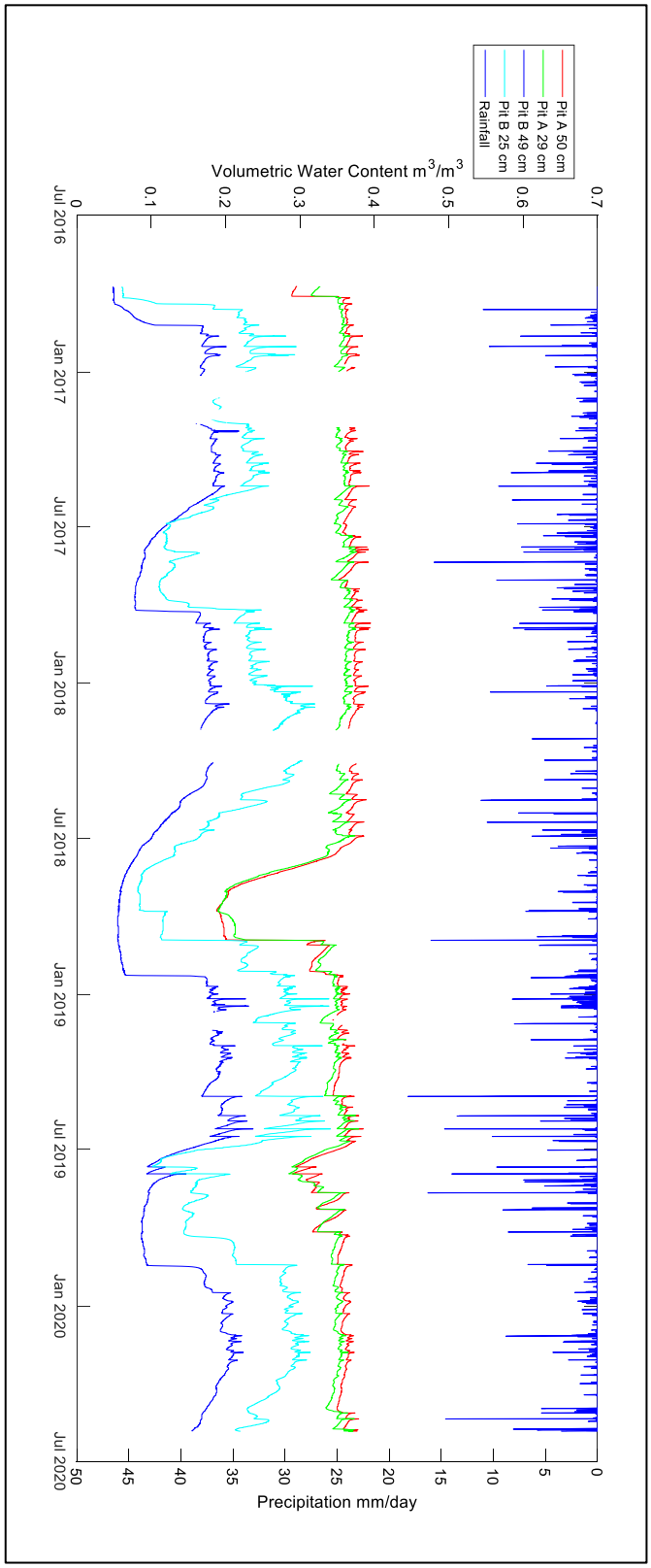

Annex 3 Water content of CS650 in soil and rainfall plot, Hermankovice

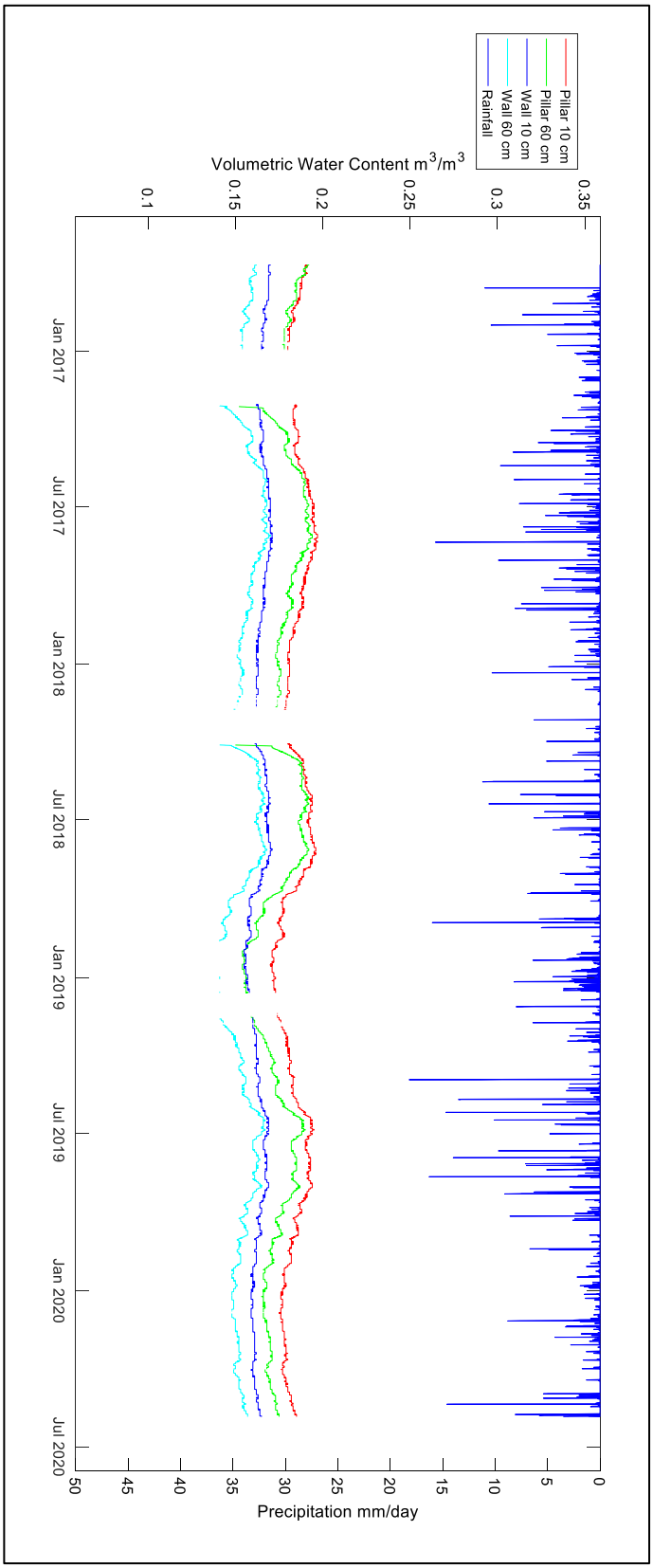

Annex 4 Water content of CS650 in the church and rainfall plot, Hermankovice

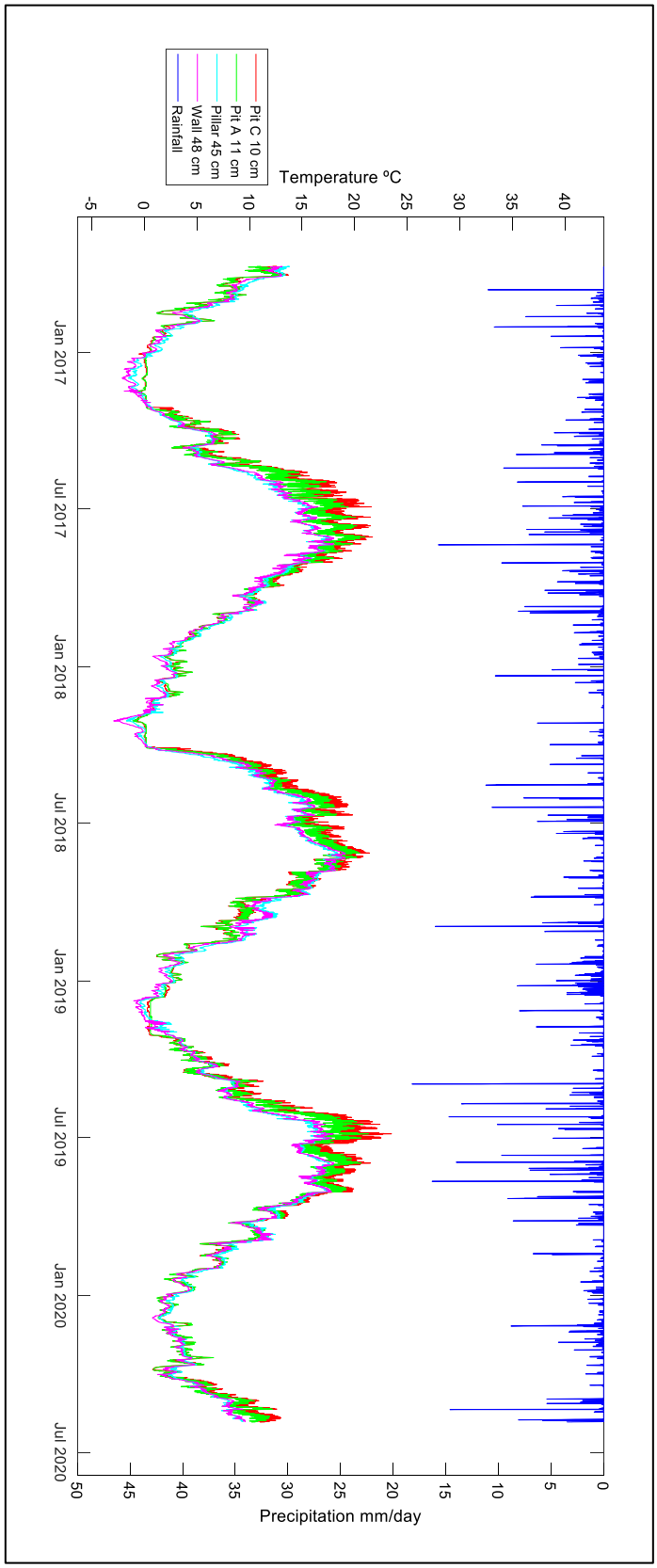

Annex 5 Temperature from MPS6 and rainfall plot, Hermankovice

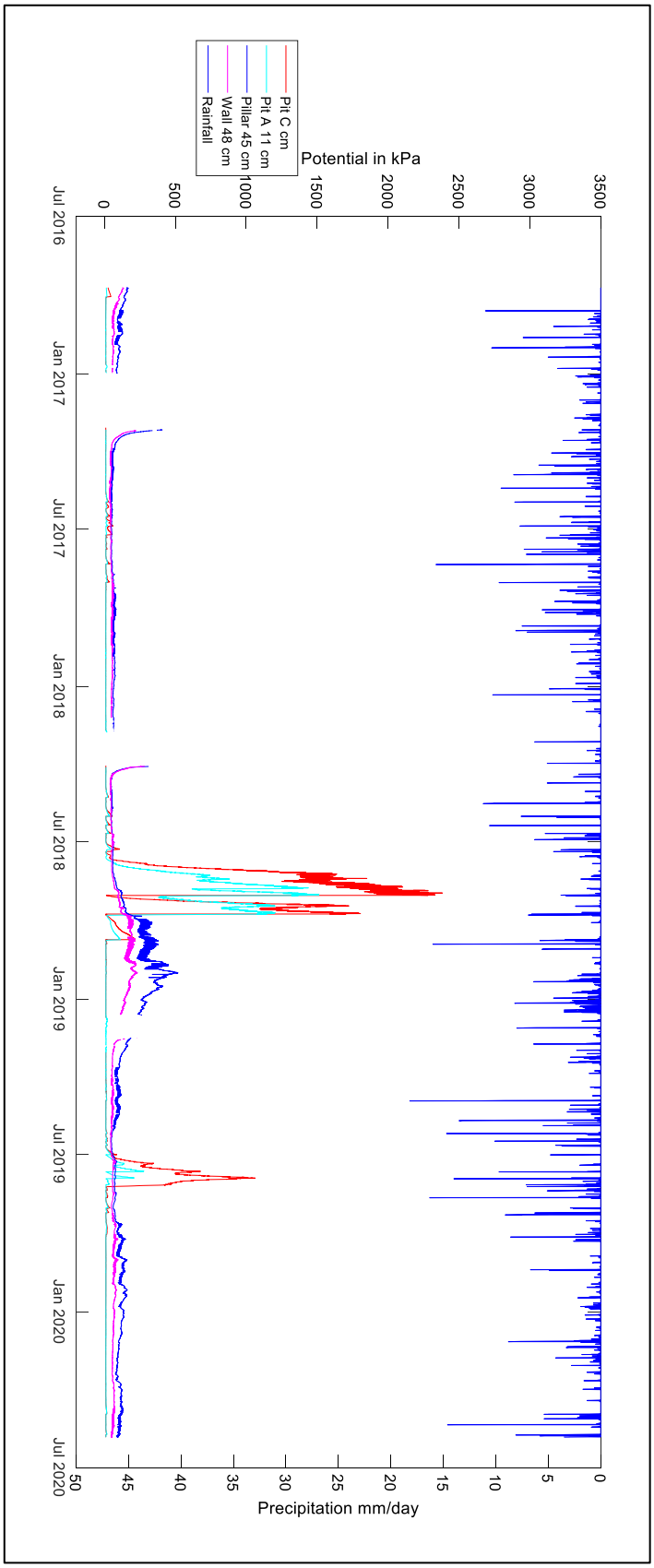

Annex 6 Pressure from MPS6 and rainfall plot, Hermankovice

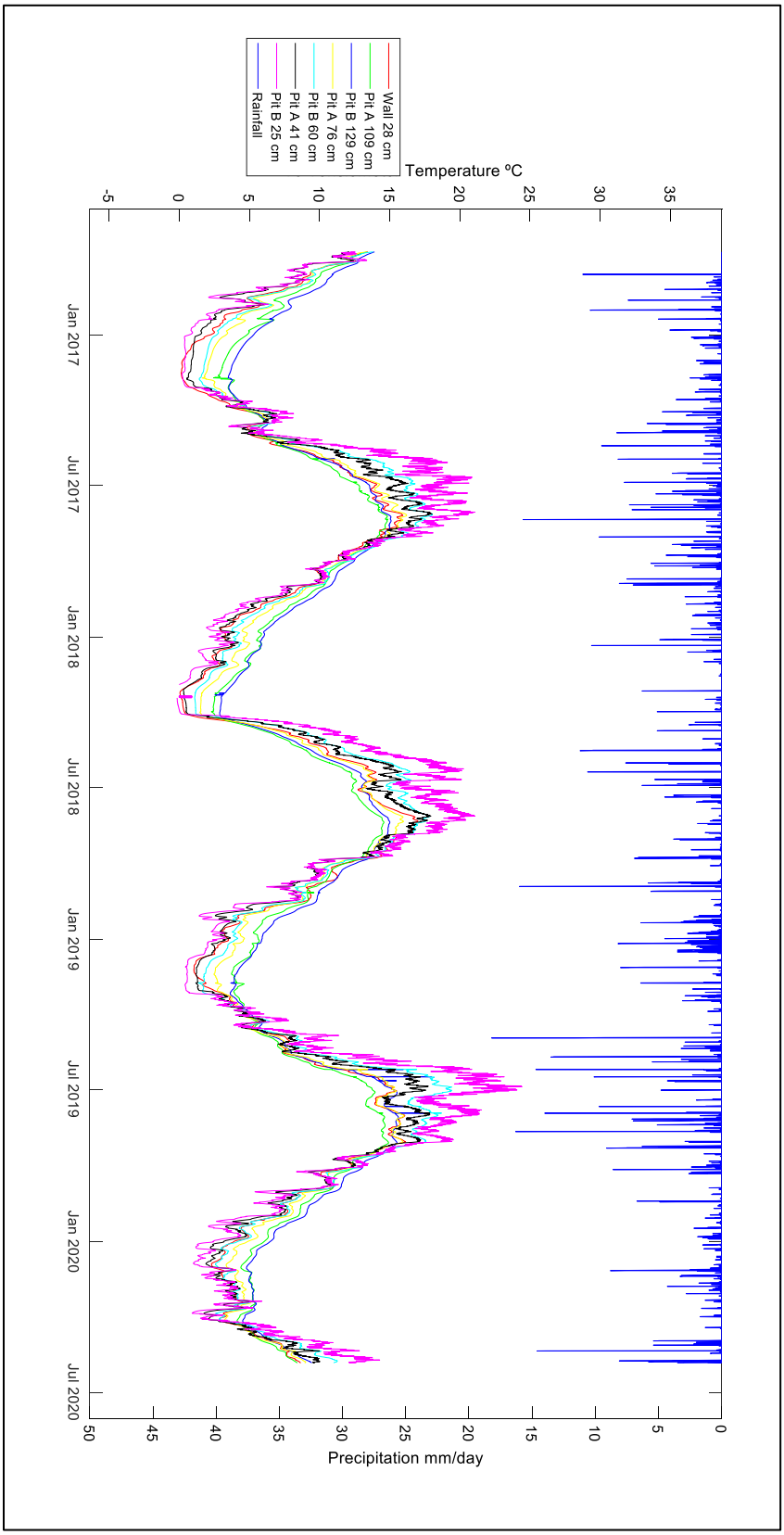

Annex 7 Temperature from T8 tensiometer and rainfall plot, Hermankovice

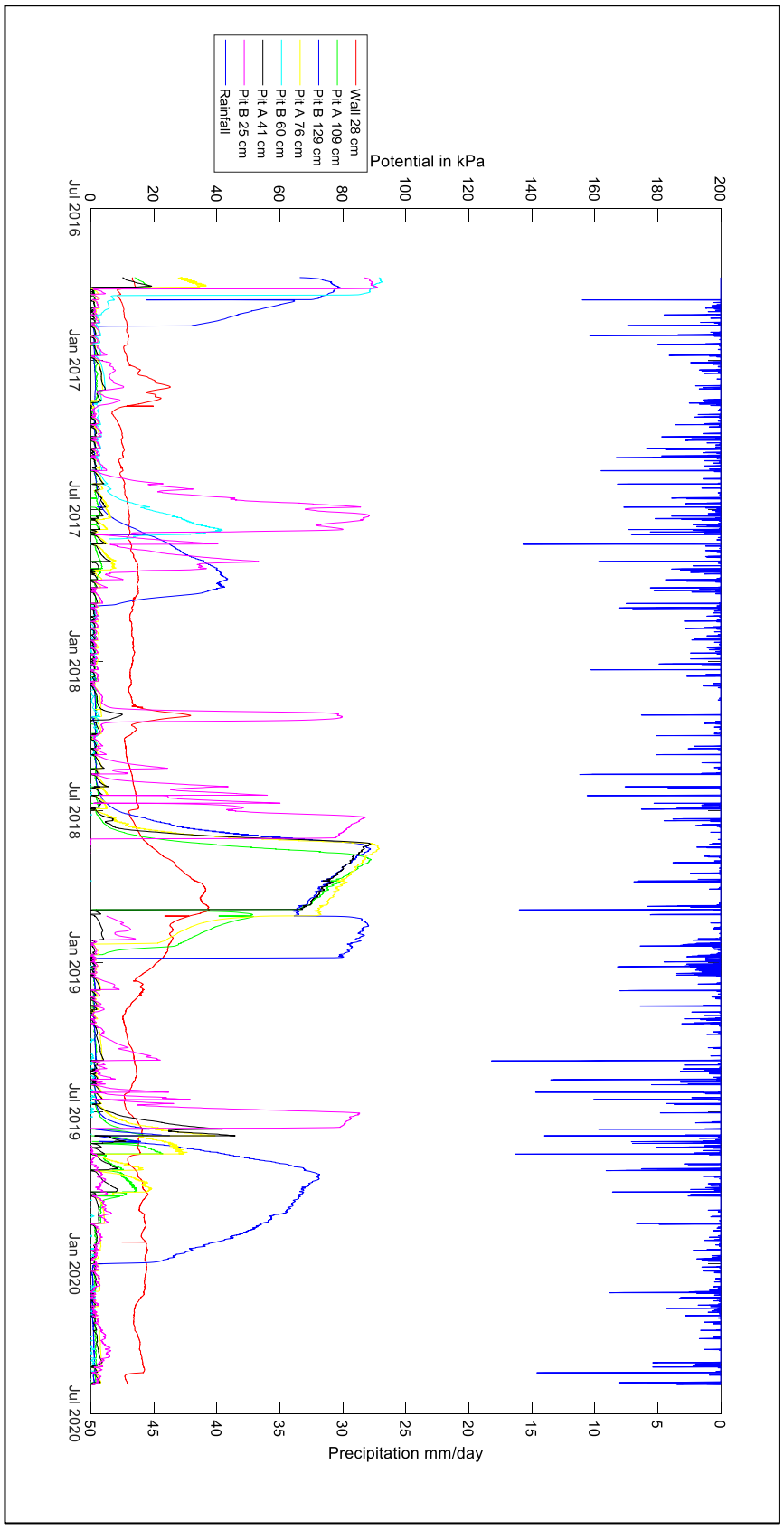

Annex 8 Potential from T8 tensiometer and rainfall plot, Hermankovice

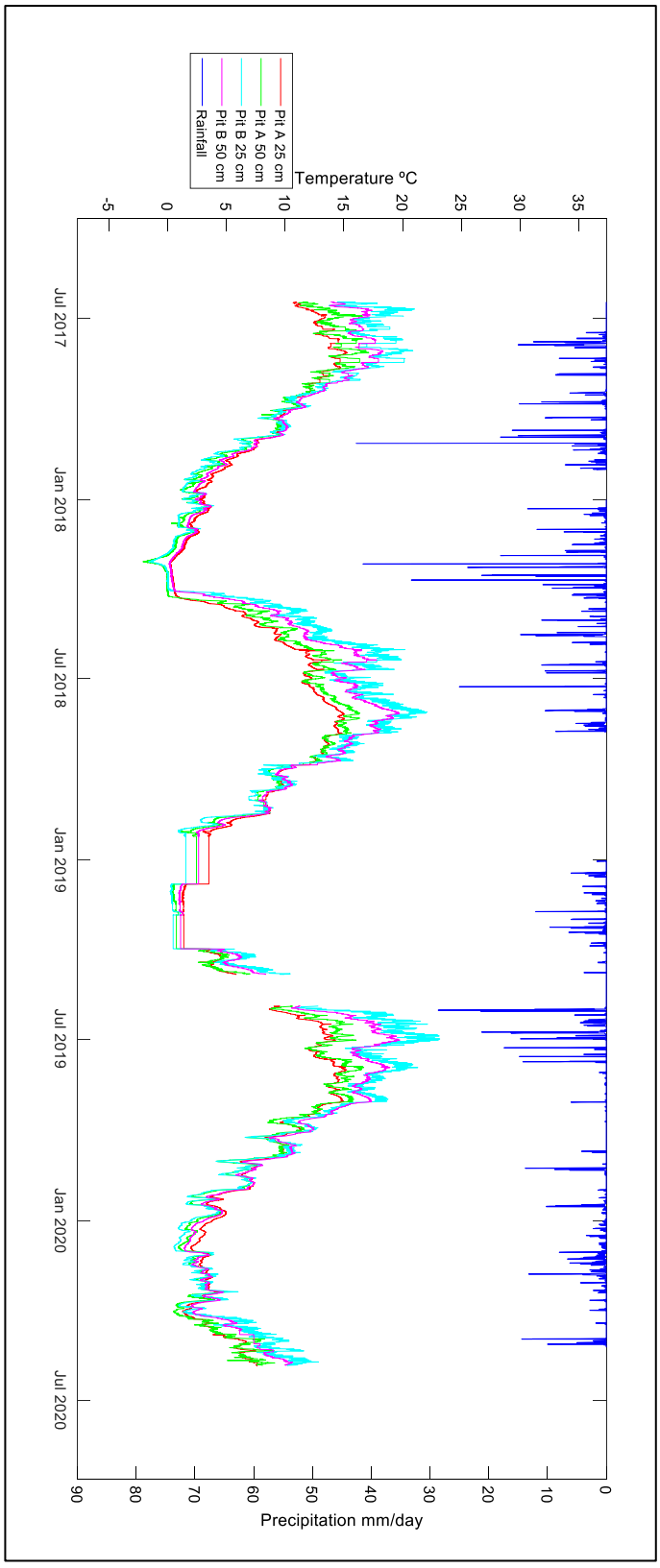

Annex 9 Temperature of CS650 in the soil and rainfall plot, Viznov

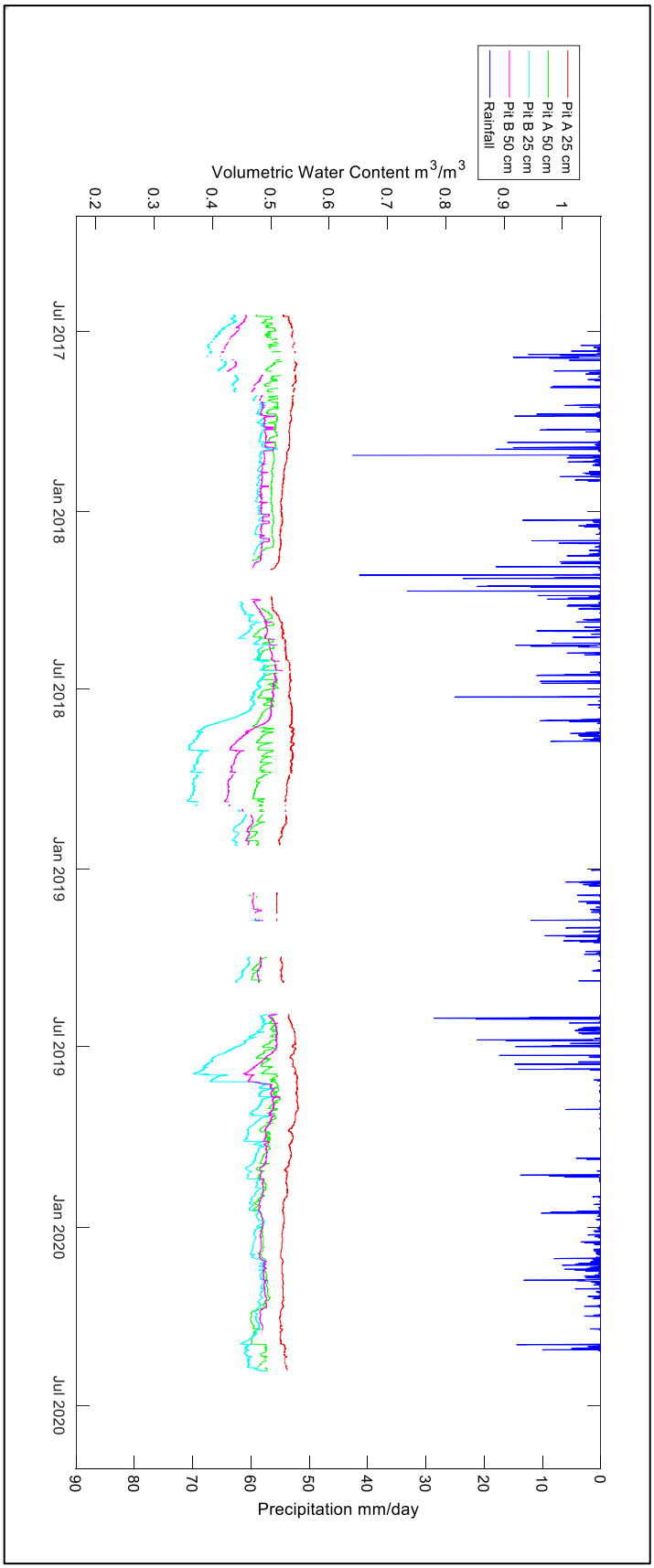

Annex 10 Water content of CS650 in soil and rainfall plot, Viznov

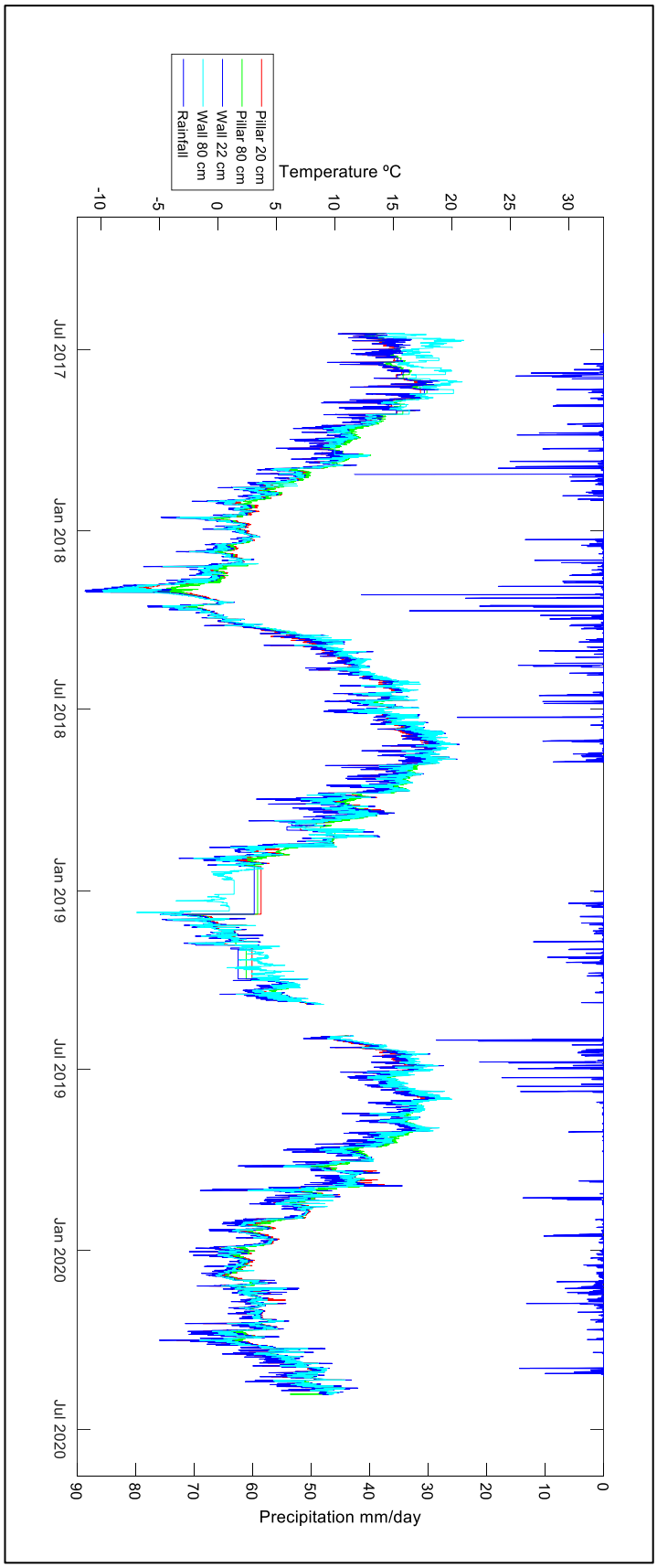

Annex 11 Temperature of CS655 in the church and rainfall plot, Viznov

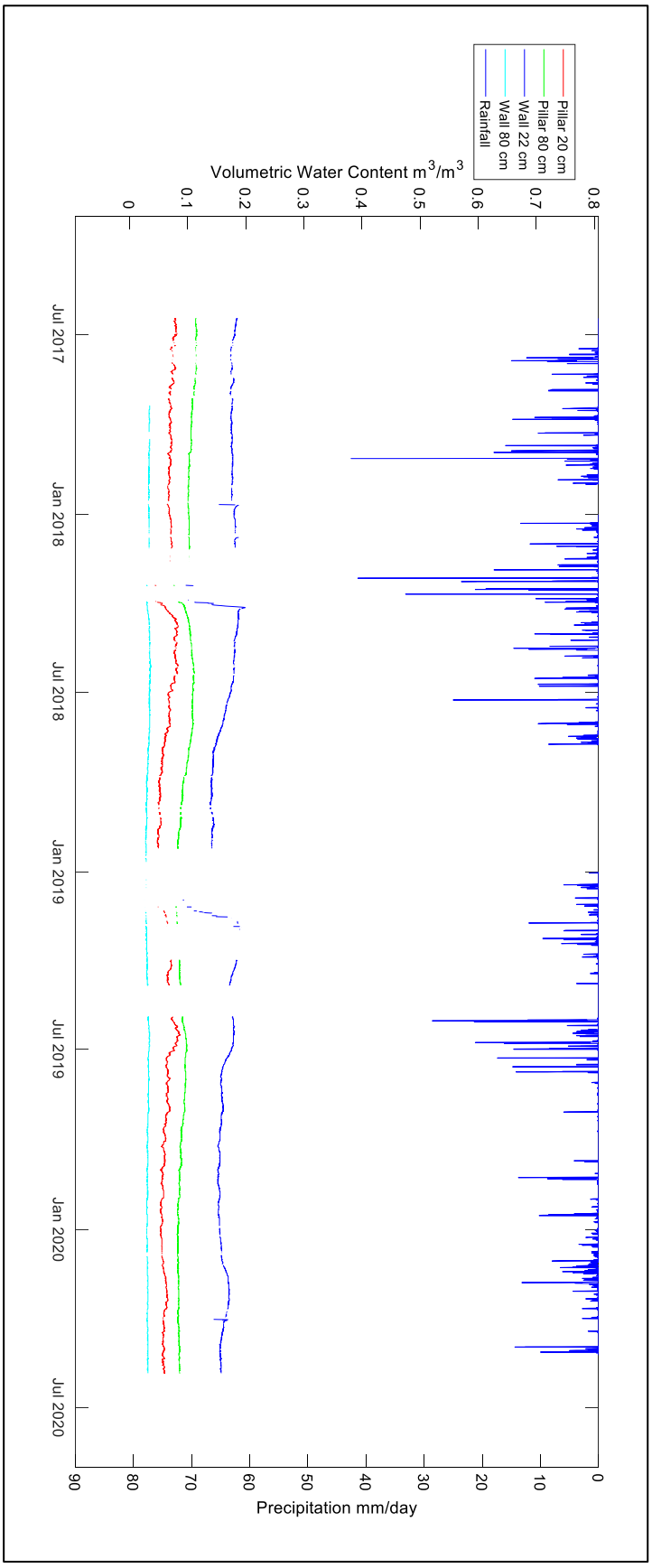

Annex 12 Water content of CS655 in the church and rainfall plot, Viznov

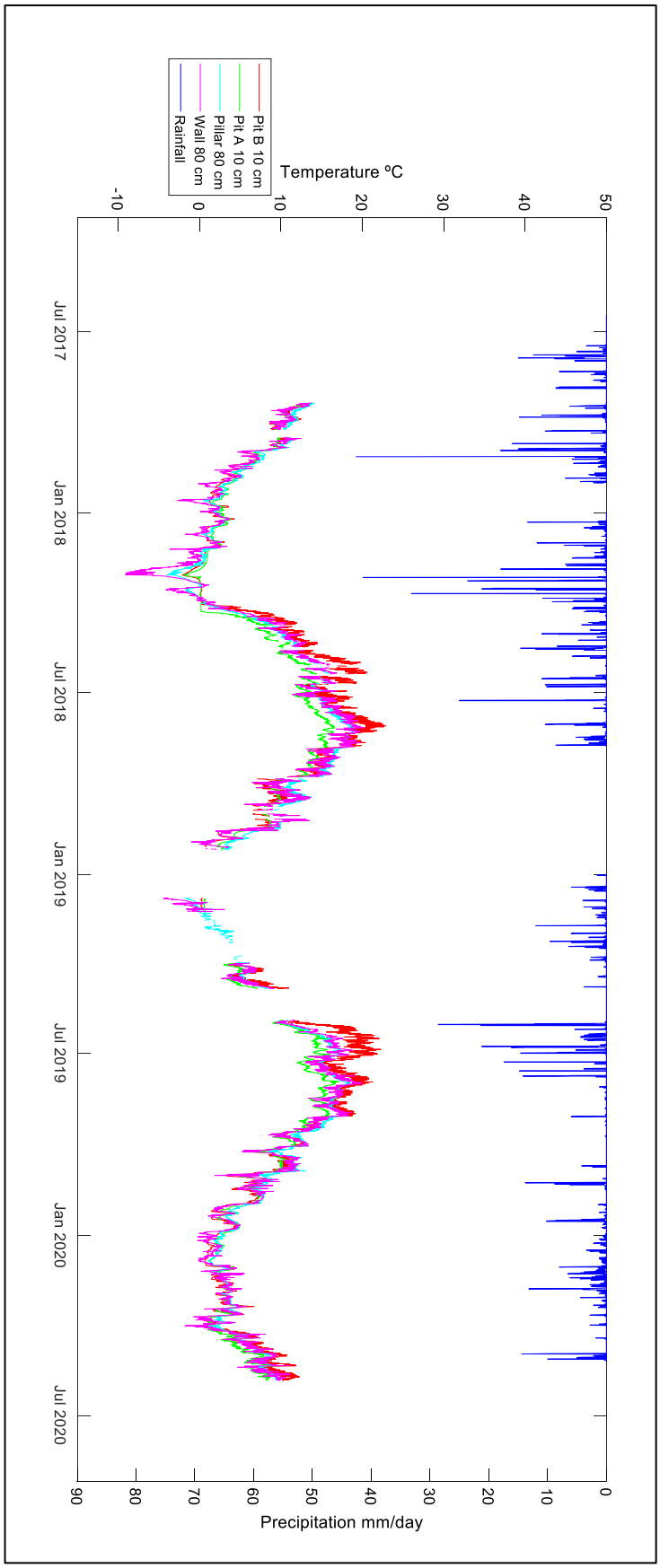

Annex 13 Temperature from MPS6 and rainfall plot, Viznov

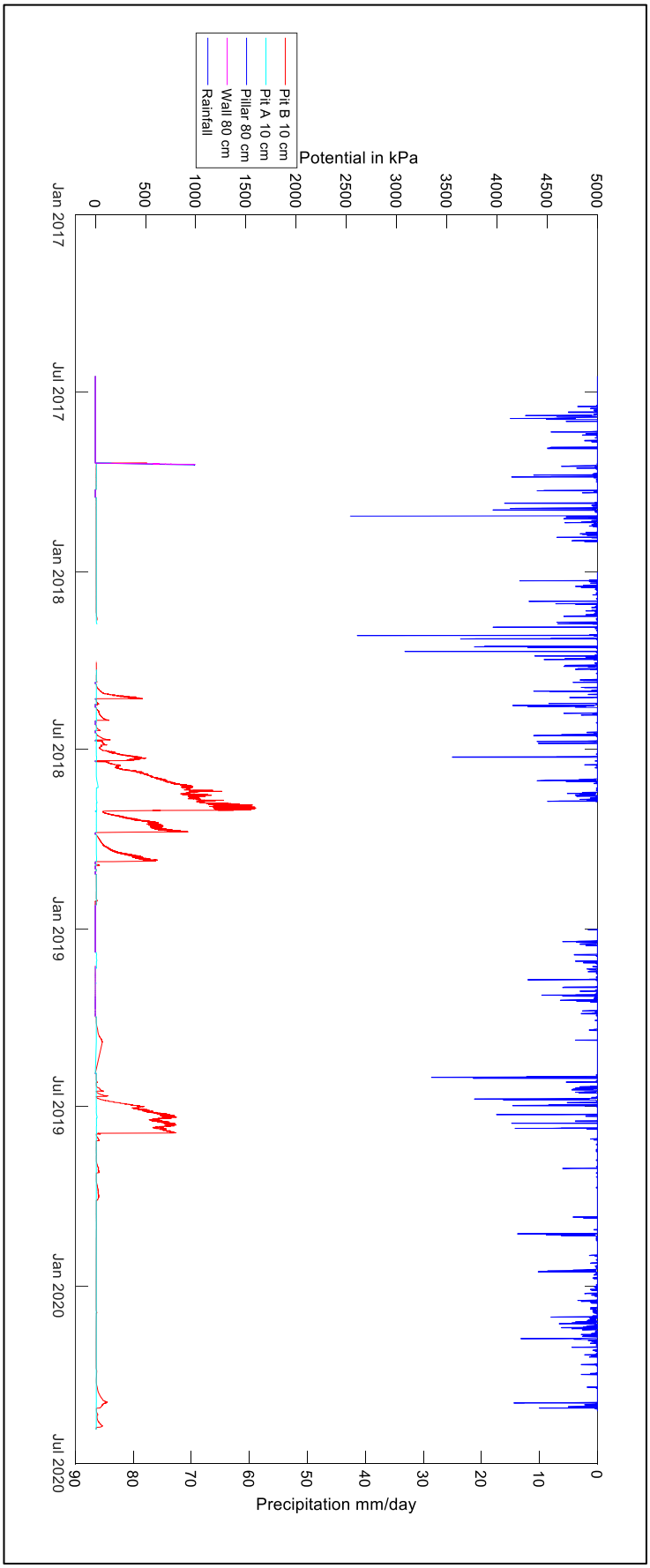

Annex 14 Pressure from MPS6 and rainfall plot, Vižňov

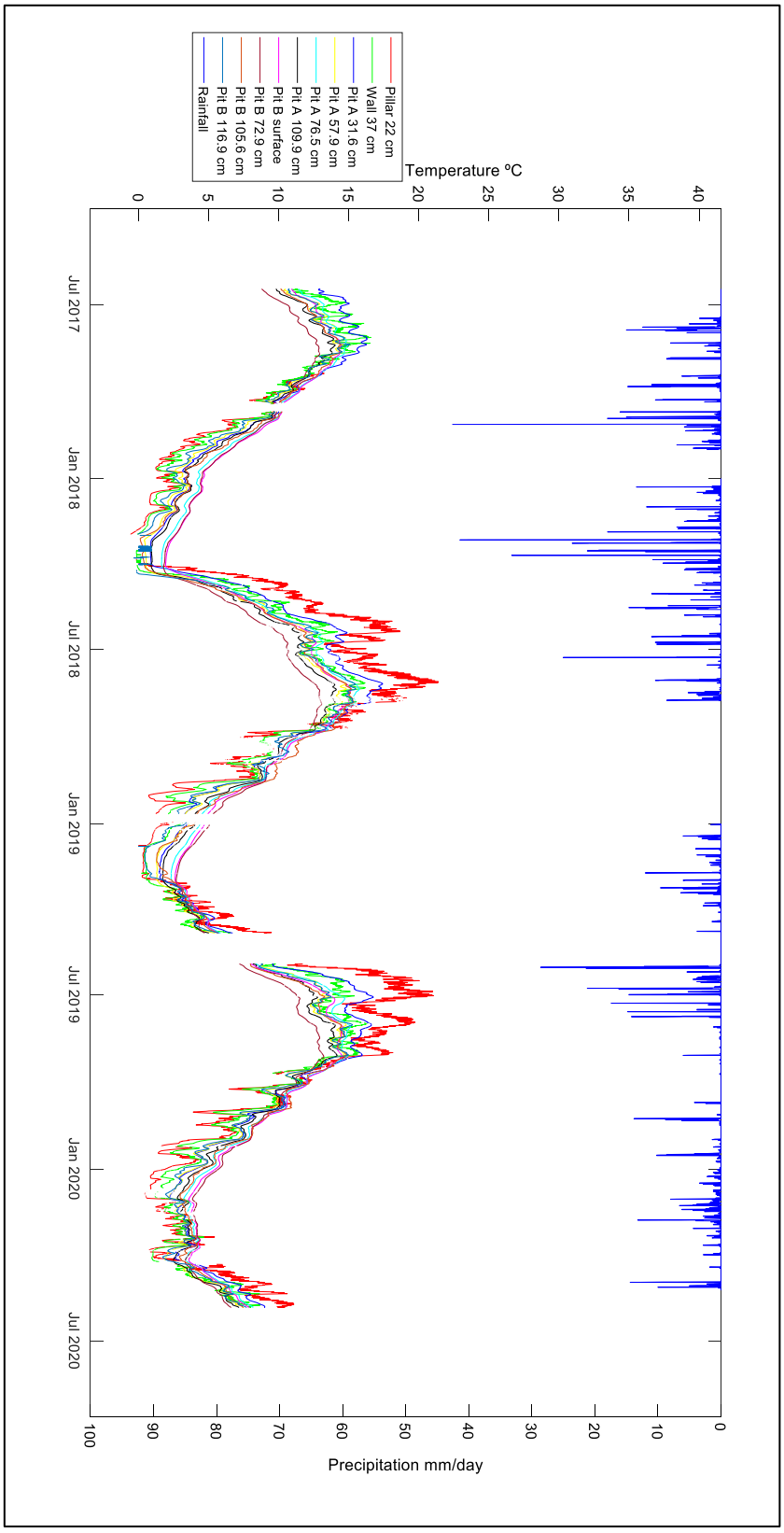

Annex 15 Temperature from T8 tensiometer and rainfall plot, Viznov

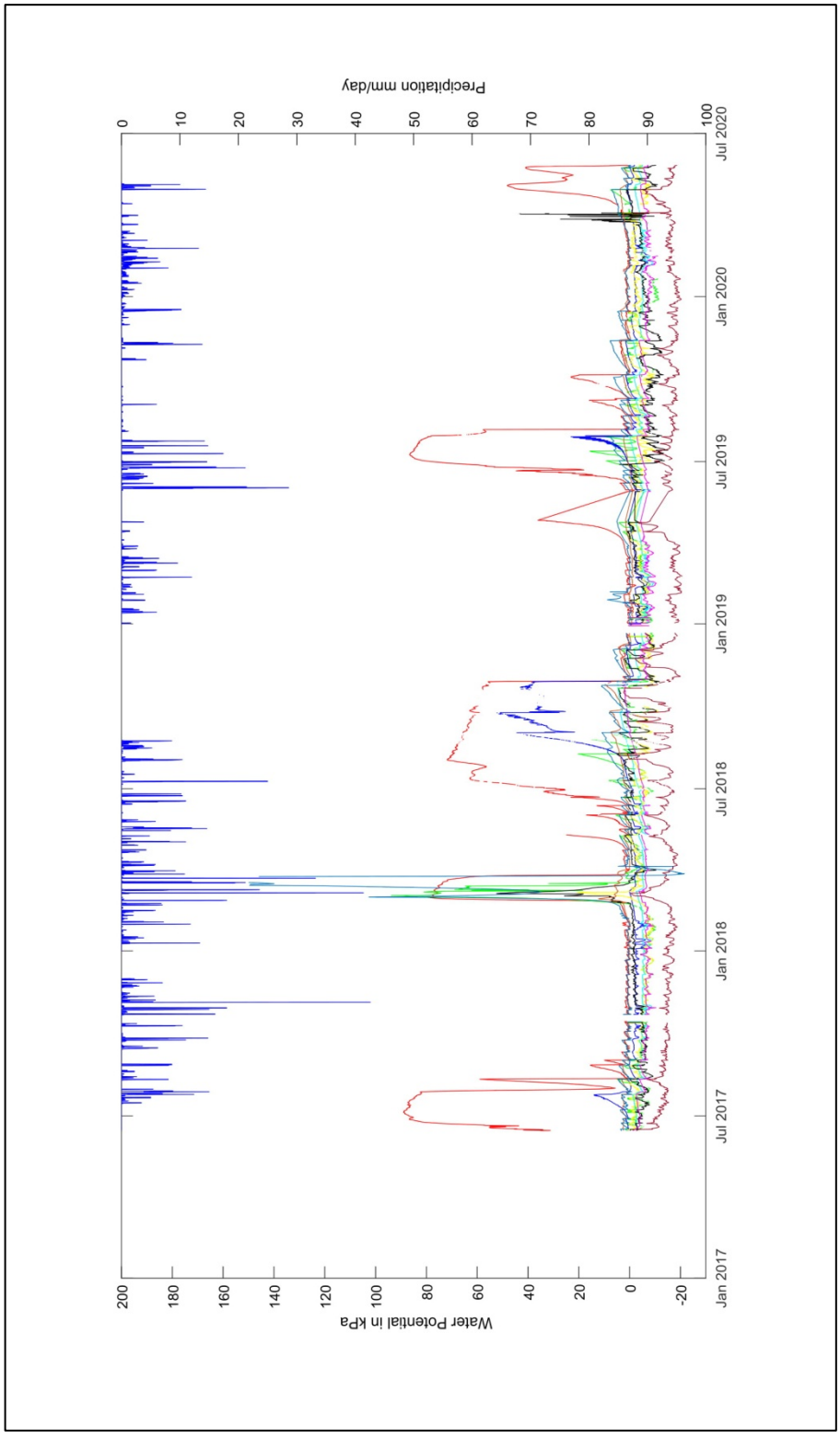

Annex 16 Potential from T8 tensiometer and rainfall plot, Viznov

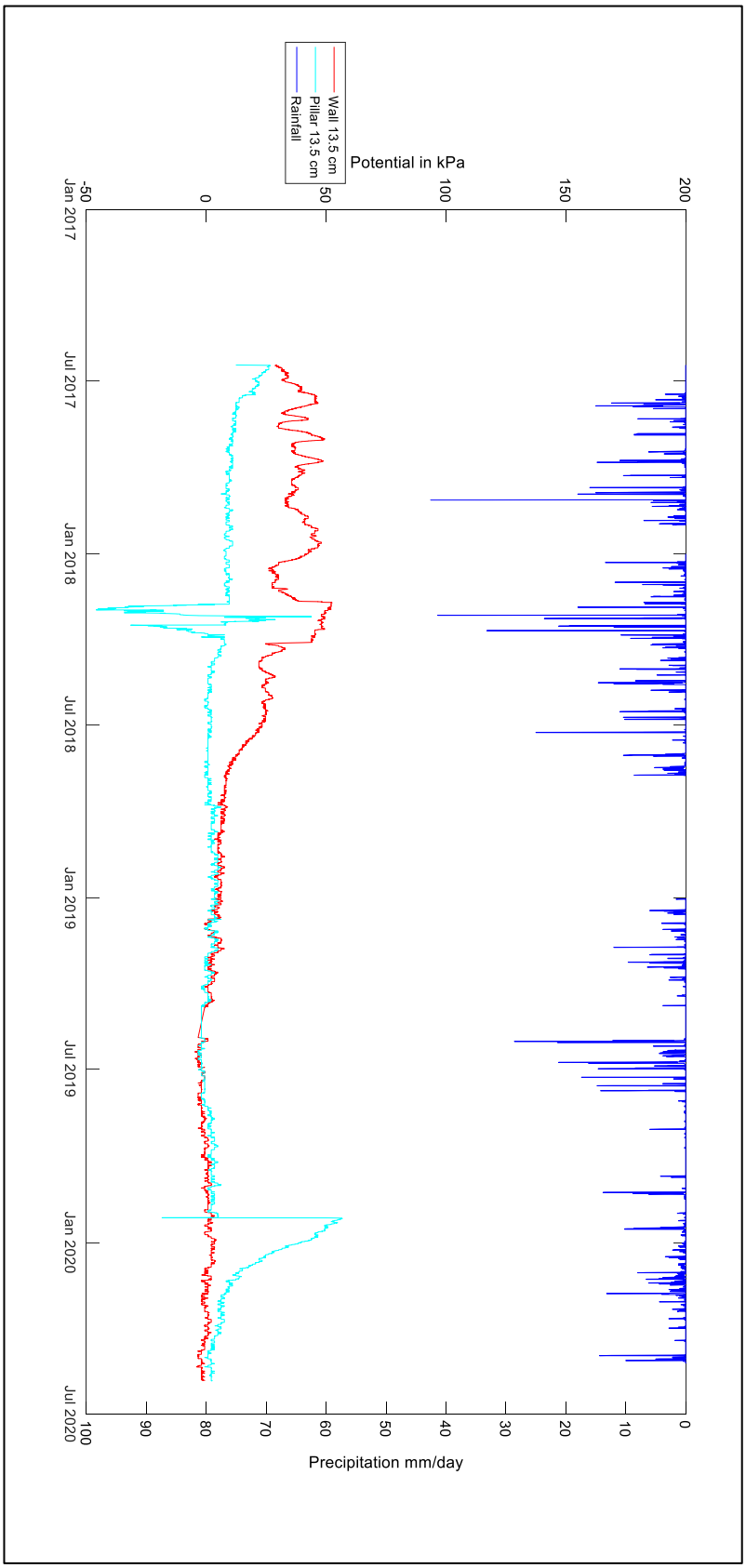

Annex 17 Potential from T5 tensiometer and rainfall plot, Viznov